

Permeable conductors for wearable and on-skin electronics

Fan Chen[#], Qiyao Huang^{#}, and Zijian Zheng^{*}*

[#] Huang and Chen contributed equally to the work.

F. Chen, Dr. Q. Huang, Prof. Z. J. Zheng
Laboratory for Advanced Interfacial Materials and Devices, Research Centre for Smart Wearable Technology, Institute of Textiles and Clothing,
The Hong Kong Polytechnic University,
Hong Kong SAR, China

Prof. Z. J. Zheng
Research Institute of Intelligent Wearable Systems (RI-IWEAR),
The Hong Kong Polytechnic University

Prof. Z. J. Zheng
Research Institute for Smart Energy,
The Hong Kong Polytechnic University,
Hong Kong SAR, China

E-mail: qihuang@polyu.edu.hk, tczzheng@polyu.edu.hk

Keywords: permeable conductors, breathability, wearable electronics, on-skin electronics

Abstract

The booming development of wearable and on-skin electronics has driven increased interest in flexible and stretchable conductors, which serve as the indispensable building blocks for these electronic devices. However, conductors for such soft electronics are mostly fabricated with impermeable elastic thin films, which not only affect the long-term wearing comfort but also limit the device's multifunctionality. In recent years, permeable conductors, conducting materials that are fabricated based on breathable materials and structures with deformability, have shown great promise for applications in wearable and skin-mountable electronics. This review provides a specific perspective on the development of permeable conductors that can simultaneously display conductivity, flexibility or stretchability, and permeability to air, moisture, and liquid. Key design considerations of permeable conductors, as well as the state-of-the-art strategies to endow flexible and stretchable conductors with permeability, are

discussed. Finally, key challenges and future directions of permeable conductors and electronic devices are discussed along with the analysis of possible solutions.

1. Introduction

In recent years, flexible and stretchable electronics have attracted tremendous attention due to their wide applications in various areas, including wearable and on-skin electronics, soft robotics, electronic skins, and implantable bioelectronics.^[1] Flexible and stretchable conductors, referring to a type of conducting components that can be bent or even stretched, are the indispensable building blocks for these devices and systems.^[2] To date, great effort has led to the development of high-performance flexible and stretchable conductors. Such conductors can either serve as the interconnectors for flexible/stretchable circuits, or function as the active electrodes for various functional devices, allowing for various electronic functions including healthcare monitoring, energy harvesting and storage, actuation, and display on human bodies and skins.^[2-3] However, in the past two decades, the research focus of flexible and stretchable electronics has been developing high-performance conductors with enhanced flexibility, stretchability, conductivity, and performance reliability. Conductors for wearable and on-skin electronics are mostly fabricated with impermeable elastic thin films.^[4] Long-term wearing comfort induced by materials and structural properties of these conductors and devices has been largely overlooked.^[5]

From the viewpoint of physiological comfort, healthy skin requires a thermal microenvironment that can provide sufficient permeability for sensible or insensible perspiration. Covering skin with impermeable materials may lead to uncomfortable sensations, increasing the risk of skin allergies and inflammation.^[6] Flexible and stretchable devices with good permeability to air, moisture, and liquid are therefore highly desirable for wearable applications, particularly for those applied in long-term on-skin health monitoring scenarios. In addition, permeability can endow the flexible/stretchable electrodes with transmission abilities to liquid or gas analytes, allowing for hypoallergenic electronic systems with high integration density of various sensing functions.^[7] Given the demands on physiological comfort and device

functionality, permeable electronics (or breathable electronics) have been proposed, in which flexible/stretchable conductors and other functional components are fabricated with permeable materials and structures.^[8] Recent studies have shown that engineering the flexible/stretchable conducting materials and structures in terms of their porosity is a promising strategy to realize permeable conductors for breathable electronics.^[9] Porous structures enabled by fibrous materials or engineered porous thin films can offer breathability to the constructed flexible/stretchable conductors, thus maximizing the physiological comfort and biocompatibility of devices on the human body.

Note that the field of wearable and on-skin electronics is expanding rapidly in recent years, and more and more permeable conductors and electronics have been reported. However, review papers highlighting the necessity of permeability for wearable and on-skin electronics and discussing strategies to endow flexible and stretchable conductors with permeability are very rare.^[5, 10] In this paper, we aim to provide a comprehensive review of permeable conductors through in-depth discussions of their design considerations, fabrication strategies, challenges, and application opportunities. The focus of this review is on the development of permeable conductors that can simultaneously display conductivity, flexibility/stretchability, and permeability for wearable and on-skin electronics. We firstly discuss the key attributes that should be taken into considerations when designing conductors for wearable and on-skin electronics. After then we focus on materials and structures that can be utilized to endow conductivity and flexibility/stretchability to inherently permeable fibrous substrates while introducing approaches that can enable permeability to those flexible/stretchable thin-film conductors. Finally, we discuss the challenges and future development directions of permeable, flexible/stretchable conductors and electronics for wearable and on-skin applications.

2. Design considerations of conductors for wearable and on-skin electronics

For device applications on human bodies, the design of electronic materials and structures needs to take both device functionalities and physiological comfort into consideration.^[6, 11] Conductors, as the essential counterparts of wearable and on-skin electronics, need to possess three capabilities: (i) permeability to gas and water to fundamentally ensure a healthy thermal microenvironment of skin/device interface so that the biocompatibility of the electronic systems can be guaranteed; (ii) flexibility or stretchability that can allow the electronic device to accommodate strains induced by the dynamic body or skin deformations without mechanical failure and noticeably sensational discomfort; and (iii) conductivity so that as-made devices can perform their electronic functions. **Figure 1a** illustrates these key design attributes of conductors for wearable and on-skin electronics, which will be elaborated on below.

2.1 Permeability

One principal function of human skin is to maintain a suitable heat and water balance of the body. Water loss from the skin surface by insensible and sensible perspirations plays an important role to control the thermoregulation of the body.^[6, 12] Under normal conditions, sweat is constantly evaporated from the skin surface to the outer environment in a form of moisture vapor at an evaporation rate of about 200~600 g m⁻² day⁻¹ for thermoregulation, even when the individual is not active.^[9, 12-13] Inefficient diffusion of moisture vapor into the environment will lead to a build-up of moisture at the skin surface and within the skin-contacted materials, which may result in uncomfortable skin sensations such as dampness and clamminess, and even skin irritation and allergy.^[6-7] Air permeability has also been proven to significantly affect the thermal comfort of the human body. Covering the skin with materials that display inadequate gas permeability will inhibit the hot air and water vapor to escape from the human body, leading to the inflammation of human skin.^[14] From the perspective of device functionality, the permeabilities of conductors to gas, moisture vapor, and liquid are also critical to ensure rapid and sensitive detection of physiological signals. In on-skin chemical sensors, analytes, such as

glucose in body secretions and volatile substances from human body odor should reach the targeting sensing electrodes, so that specific chemical or electrochemical reactions can be induced for signal detection and analysis.^[1c, 8b] The lack of gas, moisture vapor, and liquid permeabilities will limit the sensitivity of the signal detections, leading to challenges in building multi-layer integrated electronic systems.^[7]

Therefore, it is important to take the **permeabilities** to gas, moisture vapor, and liquid into considerations when designing conductors for wearable and on-skin electronic devices. Previous researches on fields of textiles and thin films have proved that permeability to air and moisture vapor is mainly dependent on the materials' geometrical structures including thickness and porosity, whereas **permeability** to moisture vapor and liquid are also closely related to the material properties.^[14a, 14b] As such, promising strategies to develop permeable conductors are to construct the conductors into thin and porous structures for moisture and air permeation, and to render these conductors hydrophilic to achieve liquid permeability.^[14b]

While the liquid permeability can be reflected by the wettability of the materials, the moisture vapor permeability is usually measured in terms of water vapor transmission rate (WVTR), that is, the amount of water vapor that passes through the materials over a specific period. ASTM E96E is one of the commonly used standard testing methods for moisture vapor permeability, in which WVTR value is measured in grams per square meter and hour (or day) ($\text{g m}^{-2} \text{hr}^{-1}$, or $\text{g m}^{-2} \text{day}^{-1}$).^[6, 15] **To ensure a healthy thermal microenvironment of the skin/device interface, it would be better to achieve the WVTR higher than $\sim 200 \text{ g m}^{-2} \text{ day}^{-1}$ for wearable and on-skin electronics. Under such conditions, the skin can breathe normally without any hindering.** Air permeability is defined by ASTM D737 standard as the rate of airflow passing through a known area at a prescribed differential air pressure between two surfaces of a material and is normally expressed as $\text{cm}^3 \text{ s}^{-1} \text{ cm}^{-2}$ (or mm s^{-1}).^[16] Both WVTR and rate of airflow can be used for

evaluating and comparing the “breathability” of different types of permeable conductors: the higher the values are, the better permeability the materials have.

2.2 Flexibility and Stretchability

Human skin is soft, and it will elongate and recover during various human motions. The skin stretch varies in different body positions, and its elongation can be up to 35~45% strain with an elastic modulus ranging from 10kPa to a few hundred kPa.^[1b, 6] Over 100% of strain can even be induced at joint areas of the human body during the movement.^[17] Therefore, electronics applied to humans are required to be flexible, or even elongated and deformed into complex and curvilinear shapes along with the body movement, while maintaining a promising level of performance and reliability that can be comparable to those of well-developed rigid electronic systems.^[1a] Due to the wide range of applications of on-body electronics, flexibility and stretchability requirements for conductors are largely varied. For example, electronic devices worn by wrists at least require bendable conductors, while achieving a successful strain sensor device for measuring the movement of body joints primarily requests a stretchable conductor that can accommodate the strain of at least 100% without mechanical failure.^[10, 17a] Super-stretchable conductors with stretching strain larger than 1,000% could further open up the applications of stretchable electronics in soft robotics or soft human-machine interactive interfaces, in which conducting stability of interconnectors over large deformations are highly important.^[18] From the viewpoint of physiological comfort to wearers, electronics built on flexible and stretchable structures/materials that have similar elastic modulus with human skin can be conformably attached to the skin surface.^[1b] This would enable the continuous monitoring of body motions and physiological signals under everyday conditions without motion restriction and sensational discomfort. Research in garment comfort has revealed that fabrics with 15~30% elongation can provide minimum resistance to body movements around

elbows, knees, and back, which could serve as a reference for designing conductors and devices for wearable and on-skin electronics.^[6]

Two main strategies have been proposed to make flexible conductors either extrinsically or intrinsically stretchable, which is illustrated in Figure 1b with representative permeable conductors. They are: (i) engineering the conductor structures to achieve extrinsically structural stretchability, and (ii) developing novel conductive materials or composites to make all the components “intrinsically stretchable”. The first approach usually involves implementing ultrathin metallic and semiconductor layers to enable flexibility and then constructing them into wavy, serpentine, kirigami, and/or mesh shapes to yield stretchability.^[3a, 19] The second approach is to develop new conducting composite materials that can simultaneously have conductive property and mechanical deformability. A general approach is to load conductive materials into an elastic matrix ((e.g., polydimethylsiloxane (PDMS), polyurethane (PU), polystyrene-block-polybutadiene-block-polystyrene styrene (SBS)) to form intrinsically stretchable conductors.^[7, 20] Such approach is capable of making one-dimensional (1D) fiber-shaped, two-dimensional (2D) planar-shaped stretchable conductors, and even printing interconnects and electrodes on flexible/stretchable substrates,^[1a, 21] which is highly necessary for the wearable/on-skin electronics that are designed to fit the complex shapes of human skin.

2.3 Conductivity

Conductivity, an electrical property that describes how easily the electrical current flows through a material, is also a key parameter for constructing permeable and flexible/stretchable conductors. The functionality of electronics highly relies on the conducting performance of the **conductors.**^[1b, 10] In actual applications, resistance, a measure of the opposition to current flow through a material, would be the important value for evaluating the electrical performance of these conductors.^[2] Since the range of applications is very broad, the conductivity and

resistance requirements of conductors are largely varied. For example, strain sensors require the conductive electrodes that could show sensitive and programmable resistance changes in response to the structural deformations (i.e., gauge factor (GF)), while current collectors for flexible energy storage devices or interconnectors for flexible electronic circuits should have high electrical conductivity and low resistance change under different mechanical deformations.^[10, 22] Therefore, developing different conducting materials and their composites is mostly to engineer their conducting performance to satisfy different requirements of conductors in wearable and on-skin electronics.

Conductive materials that are commonly used for constructing flexible and stretchable conductors include metal (e.g., silver (Ag), copper (Cu), gold (Au)) thin films, metal nanoparticles (NPs) and nanowires (NWs), carbon-based nanomaterials (e.g., carbon nanotubes (CNTs), graphene, reduced graphene oxide (RGO)), conducting polymer (e.g., polyaniline (PANI), polypyrrole (PPy), and Poly(3,4-ethylenedioxythiophene):poly(styrene sulfonate) (PEDOT:PSS)), ionic liquids, liquid metal alloys (LM), and conductive hydrogels. Due to the high electrical conductivity ($\sim 400,000 \text{ S cm}^{-1}$), metal thin films are usually constructed into structurally flexible forms and are widely used for interconnects and electrodes for flexible/stretchable devices.^[3a, 19] Metal and carbon-based nanomaterials, as well as conducting polymers, can be functioned as conducting fillers and be incorporated with polymeric matrix to form coated or composite conductors.^[20b, 23] As such, the conducting performance is closely related to the conducting network formed on/within the polymeric matrix, providing a possibility to engineer the conductors' electrical and mechanical properties for specific requirements.^[24] Ionic liquids is a kind of organic salts with a low melting temperature (usually below $100 \text{ }^\circ\text{C}$) and high ionic conductivity (within 10^{-4} to $10^{-2} \text{ S cm}^{-1}$ around room temperature).^[25] Their physicochemical properties can be flexibly tuned by the choice of anion-cation pairs, leading to wide application possibilities as ionically conductive electrolytes in

advanced electrochemical devices such as electrochemical energy storage or power devices, dye-sensitized solar cells, and fuel cells.^[26] LMs are liquid-state conductive materials with high stretchability (infinite) and conductivity ($> 10^4 \text{ S cm}^{-1}$). Recent studies have revealed that gallium (Ga) metal-based LMs, including EGaIn (Ga alloyed with Indium (In)), and Galinstan (Ga alloyed with In and Tin (Sn)), have the advantages in low toxicity, high electrical conductivity ($\sim 34,000 \text{ S cm}^{-1}$), and high thermal conductivity.^[4a, 27] They have been investigated as promising conducting materials for stretchable interconnects, antennas, soft robotics, and bioelectronics.^[28] Conductive hydrogels are formed by a hydrophilic network of 3D crosslinked natural or synthetic polymers and introduced with electrically or ionically conductive materials. Such hydrogel-based conductive materials are intrinsically stretchable ($>1,000\%$), biocompatible, and viscoelastic, making them promising for biocompatible electronic applications, such as sensors, actuators, and artificial soft tissue.^[23e, 29] Noted that in this review, only the representative conductive materials are highlighted to illustrate how current approaches have been adopted to realize the permeability of flexible/stretchable conductors. Details on conducting materials are discussed in recent reviews focusing on materials for stretchable conductors.^[2, 24, 29c]

In summary, taken the device functionalities and physiological comfort into consideration, conducting performance of the conductors should be realized based on flexible/stretchable materials in porous forms. As such, the as-developed conductors can provide promising flexibility/stretchability, conductivity, and most importantly, maintain the permeability to air, moisture vapor, and liquid. **It should be also noted that these conductive, flexible/stretchable, and porous materials need to be biocompatible to avoid immune reactions,^[5] which is the prerequisite for electronics mounted on human skins or worn by human bodies.** Strategies to endow high-performance conductors with both permeability and flexibility/stretchability will be discussed in Section 3.

3. Strategies to engineer conductors permeable, flexible, and stretchable

In a broad term, the development of flexible and stretchable conductors with permeability largely relies on engineering the materials and structures of conductors in terms of their porosity. The main ways for achieving flexible and stretchable conductors with permeability, in practice, are (i) using fibrous materials, and (ii) engineering the porosity of thin-film conductors.

3.1 Fibrous conductors

Fibrous materials are referred to as assemblies of fibers that have a high aspect ratio (>50) with a thickness (or diameter) ranging from several hundreds of nanometers to several millimeters. They are inherently porous with various levels of porosity up to 99% and have softness and deformability, thus exhibiting the nature of breathability, flexibility, and even stretchability.^[14c] With these appealing features, fibrous materials have been demonstrated as one of the substrate materials for permeable conductors. Depending on the structures of fiber assemblies, conductors made from fibers, i.e., fibrous conductors, can be classified into three categories: (i) 1D fiber/yarn-shaped conductors, (ii) 2D fabric-shaped conductors, and (iii) nanofiber-mat-based conductors.

3.1.1 1D fiber/yarn-shaped conductors

Flexible and stretchable conductors in fiber or yarn (i.e., a strand of fibers) configuration can exhibit advantages in lightweight, inherent breathability, and greater adaptability to the frequent deformations of the human body during usage. Benefiting from the 1D assemblies, these fibrous conductors with sufficient length can be directly integrated into existing clothes or formed into a fabric, while the permeability and flexibility/stretchability can well retain.^[21b] Typical fabrication approaches for flexible and stretchable conductive fibers/yarns are based on coating conductive materials around the surface of polymeric fibers, or the formation of composite

fibers that consist of conductive materials and insulating flexible/elastomeric materials. Note that this section only discusses the very typical fabrication methods that can be utilized to scalably develop flexible or stretchable fiber/yarn conductors for wearable integration. Practically, the combination of different fabrication methods is often utilized to achieve satisfactory conducting and mechanical performance.

Coating for fiber/yarn conductors

Coating has been regarded as the simplest fabrication process to endow conductivity to flexible and stretchable materials. In a typical coating process, conductive materials are either physically dip-coated, brush-coated or wrapped onto the polymeric fiber strands,^[21b, 30] or incorporated into fibers in a bottom-up way through chemical reaction processes.^[31] Stretchability can be achieved by either using elastic fibers as a core or utilizing the “pre-strain” strategy.^[32] For example, Wang et al.^[32d] developed the stretchable conductive yarn by dip-coating the **single-walled CNT(SWCNT)** ink onto an elastic cotton/PU core-spun elastic yarn (Figure 2a-c). Such stretchable conductive yarns could sustain the tensile strain up to 300% and exhibit long-term cycling stability for nearly 300,000 stretching cycles without noticeable breakage, which could be used as electrodes in strain sensors for human motion detection. He et al.^[33] reported a **highly stretchable PPy-coated thermoplastic PU (TPU) fiber that was made by *in-situ* confined polymerization of a PPy coating in an elastomeric TPU fiber network. The as-prepared PPy-TPU fibers could possess excellent stretchability up to 1450% in strain and promising sensitivity to both temperature changes and tensile strains, which could be woven into fabrics and applied as temperature and strain sensors to alarm the accident fall for aged peoples.**^[33] Liu et al.^[32f] wrapped CNT sheets along the longitudinal direction of the pre-stretched rubber fibers (Figure 2d). After releasing the strain of the fiber, distinct short- and long-period sheath bulking that occurred reversibly out of phase around the fiber surface (Figure 2e) enabled a very small

resistance change of less than 5% even under 1,000% strain, which is appealing to be used as the stable interconnects for elastic electronic circuits.

Nevertheless, adhesion between the conductive sheath and flexible/elastic fiber core is an important issue when designing flexible/stretchable fiber strands with a conductive coating. Poor adhesion of conductive coating (particularly the metallic layer on soft fiber) will lead to the mechanical instability of the conductors, thus limiting the flexibility/stretchability and the stability of yarn electrodes for long-term applications. Zheng and his coworkers proposed a polymer-assisted metal deposition (PAMD) strategy to address this issue.^[34] In this method, the interfacial polymer grafted on the fiber surface was utilized as an anchoring layer to ensure that the metal could be firmly adhered onto the fiber substrate and enhance the mechanical durability upon large deformation.^[35] Liu et al.^[36] recently reported a breathable and stretchable strain sensor that was constructed by embroidering the elastic yarns and PAMD-developed conductive yarns (Figure 2f). Taking advantage of the high electrical conductivity ($\sim 0.23 \Omega \text{ cm}^{-1}$) and stability of the Cu-coated conductive yarns achieved by the PAMD approach, the as-embroidered strain sensor revealed outstanding sensitivity to tensile strain (gauge factor = 49.5 in the strain of 0~100%) and durability (3,000 stretching cycles). More importantly, the sensor made with inherently breathable conductive yarns could possess superior permeability to moisture ($24 \text{ g m}^{-2} \text{ h}^{-1}$) and air ($150 \text{ cm}^3 \text{ s}^{-1} \text{ m}^{-2}$), which is critical for realizing wearing-comfort and high-performance strain sensors.

Direct spinning of fiber/yarn composite conductors

Great research efforts have also been made on developing novel stretchable 1D composite conductors based on the direct spinning of conductive and elastic materials composites.^[21b] Among many spinning methods, wet spinning^[37] and thermal drawing,^[38] have been widely

applied for the extrusion of elastomeric matrix and conductive materials to form stretchable fiber/yarn composite conductors.

Wet spinning is one of the conventional production technologies for filament yarns, in which filament yarn can be formed by instantly injecting a polymeric solution through a nozzle into a coagulation bath. By adding conducting fillers into the elastomeric polymer solution, stretchable conductive yarns can be formed.^[21b] Seyedin et al.^[39] utilized this scalable wet-spinning technique to scalably produce $\text{Ti}_3\text{C}_2\text{T}_x$ MXene/PU composite fibers with conductivity and high stretchability for strain sensing (Figure 2g). With MXene fillers in the PU filament matrix, the fiber showed a large sensing range of $\approx 152\%$ with a high gauge factor of 12,900. It was also demonstrated that the sensing range could be further improved to $\approx 175\%$ by producing the fiber with MXene/PU sheath and pure PU core via a coaxial wet-spinning process (Figure 2h). Similarly, stretchable fibers with Ag NPs/PU,^[20c] CNT/MXene/PU,^[40] and Graphene/SBS^[41] composite materials, and CNT-silicone rubber^[42], SWCNT-thermoplastic elastomer (TPE),^[43] and SBS-SBS/CNT core-sheath structures^[44] have also been demonstrated in the literature. In addition, hydrogel materials are also appealing for making stretchable fiber/yarn conductors. Via the wet-spinning process, ionic/electrically conductive materials can be physically added or chemically crosslinked with the hydrogel network to form a conductive pathway, followed by spinning into a hydrogel-based ionic-/electrically conducting fibers.^[29c] For example, Chen et al.^[45] developed a strain-sensitive conductive hydrogel fiber by wet-spinning of the RGO-doped poly(2-acrylamido-2-methyl-1-propanesulfonic acid-co-acrylamide (RGO-poly(AMPS-co-AAm)) hydrogel (Figure 2i). The addition of RGO and the presence of propanesulfonic acid groups in AMPS respectively enable electronic conduction and ionic conduction of the as-spun hydrogel fiber. The hydrogel fiber could be stretched beyond 300% with a sensitive resistance change in response to the strain (Figure 2j). ECG

signals could be clearly recorded by attaching the RGO-poly(AMPS-co-AAm) hydrogel to the skin surface of the wrist, verifying the good conductivity of this hydrogel (Figure 2k).

Thermal drawing is another popular technique for making flexible/stretchable 1D-shaped conductors. In this manner, the fiber can be continuously extruded by passing a preform of filament into a furnace, where the preform is softened or melt and then drawn into a thin fiber with controllable size.^[21b, 32b] Structures and components of the thermally drawn fibers can be readily controlled by adjusting the preforms, through which fibers/yarns with multi-materials and structures can be formed.^[46] Dong et al.^[47] used thermal drawing process to developed kilometer-long elastomer fibers from a single preform that was combined with a thermoplastic elastomer (Geniomer) sheath and multiple cores of LM (Ga) (Figure 2l-m). Taking advantage of the stretchability of the elastomeric sheath as well as the deformability and conductivity of the LM core, the resulting fibers were able to sustain complex deformation and elongations up to 560%, thereby allowing for efficient energy harvesting from mechanical friction or vibration (Figure 2n). Fink group advanced the thermal drawing method for the full integration of various types of fiber-based devices, in which the geometries of all the functional components were customized into a preform and then drawn into microfibers.^[46c, 48] Recently, Fink and his coworkers achieved 100-meter-long supercapacitor fibers through the thermal drawing system.^[49] A macroscale preform consisting of an electrode, electrolyte, conductive polymer, metal current collectors, and encapsulation cladding was thermally drawn into a fully functional energy-storage fiber (Figure 2o). These thermally drawn fibers exhibit the energy density of $306 \mu\text{Wh cm}^{-2}$ at 3V and the 100% capacitance retention over 13,000 charging/discharging cycles at 1.6V. They have sufficient flexibility and tensile strength for the application in the machine-weaving of fabrics and 3D printing (Figure 2p). This methodology potentially can facilitate the fabrication of multifunctional flexible/stretchable yarns at a large scale, thereby

allowing the direct and seamless integrations of fiber-based devices into existing clothing without affecting the breathability and wearability.

3.1.2 2D fabric-shaped conductors

1D fiber/yarn-shaped conductors can be further constructed into a piece of fabric to achieve a 2D fabric-shaped conductor. Their fibrous nature and fabric structure can ensure the flexibility and permeability of the as-made fabric conductors while endowing electric functionality to the clothing and garments.^[50] For example, Zhao et al.^[51] developed a series of breathable **trioelectric nanogenerator** (TENG)-based pressure sensors manufactured by weaving, knitting, and stitching of Cu-coated and parylene/Cu-coated yarn electrodes, which could sensitively detect the grip posture (Figure 3a). All the sensing fabrics maintained similar air and moisture permeability to those of commercial fabrics, demonstrating the promise in wearable electronic applications (Figure 3b-c). Recently, Chen, Peng, and their coworkers reported a flexible, stretchable, and breathable large-area display textile (600 x 25 cm²) containing 50,000 electroluminescent units, which were achieved by weaving conductive weft and luminescent warp yarns (Figure 3d-g).^[3b] Further weaving with other electronic system components, including keyboard and power supply, could achieve a fully textile-based electronic system, demonstrating the system's application promise in various areas such as healthcare and communication (Figure 3h).^[3b]

Other than integrating fiber/yarn conductors into fabrics to form fabric-shaped electrodes, fabric-shaped electrodes can also be fabricated by utilizing existing 2D assemblies of fibers, i.e., fabrics. In general, direct coating of conductive materials into pristine fabrics, carbonization of fabrics, and printing/patterning of conductive pathways onto pristine substrates can all realize permeable 2D fabric-shaped conductors.

Coating for fabric conductors

Similar to fiber/yarn conductors that are made by coating techniques, conductive fabrics can be produced by coating the non-conductive fabric with conductive materials. To date, coated conductive fabrics have been extensively developed and reported in the literature, such as CNT-coated cotton fabrics,^[52] graphene-coated fabrics,^[53] Ag nanowires-coated cotton fabrics,^[54] conducting polymer-coated textiles,^[55] and Ag-/Ni-/Cu-coated textiles.^[56] As only a thin layer of conducting materials is applied to the fabrics, coating usually does not affect the breathability and flexibility/stretchability of the fabrics. Hsu et al.^[54b] demonstrated a personal thermal management system by applying metallic NWs-coated woven fabric (Figure 4a). The coating of Ag NWs could not only reflect the human body's infrared radiation for thermal insulation but also allow for Joule heating to provide extra warmth. In addition, the moisture permeability of the original fabric was not sacrificed, which was only reduced by 2% for Ag NWs coating (Figure 4b). Lu et al.^[56a] combined the electroless deposition and electrodeposition techniques for the fabrication of stretchable knitted-fabric conductors (Figure 4c). Such a solution-based process could achieve the loading of conducting layer around individual fibers, thereby retaining the fibrous structure and corresponding comfort of the original textiles (Figure 4d). Stretchable heater patches fabricated by such metallic knitted fabrics showed reliable temperature distribution without obvious deterioration in both static and dynamic states when they were applied on fingers and wrist, demonstrating the potential application of such metal-coated conductive textile in wearable thermotherapy (Figure 4e).

Carbonization of fabrics

Under a high-temperature annealing process, fabrics, such as cotton, hemp, silk, and acrylic fabrics can be directly converted into conductive carbon fabrics, in which the fibrous and woven/knitted structures can be well maintained.^[57] For example, Li, Zheng, and their coworkers directly converted the hemp knitted fabrics into a graphited state at an 800°C

annealing temperature with a nitrogen atmosphere to endow the electrical conductivity (Figure 4f).^[57a] Such carbon fabric conductors could possess remarkable static and dynamic stability under different applied pressure, showing the promising application as the sensitive pressure sensor for the detections of human physiological signals and body movement. More importantly, the fibrous and knitting structure enabled the fabric conductor to have a high air permeability ($600 \text{ cm}^3 \text{ s}^{-1} \text{ cm}^{-2}$) and high water-vapor permeability ($40 \text{ g m}^{-2} \text{ h}^{-1}$), allowing complete perspiration and significantly improving the wearing comfort (Figure 4g-h).

Printing/patterning of conductive pathway on fabric substrates

The above-discussed approaches are to endow conductivity to flexible/stretchable fabric by converting pristine fabrics into conductive composite conductors, which have limitations in pattern diversity. Printing technology is considered a promising technology to offset this patterning limitation, through which conductive materials are prepared as ink forms and “pasted” onto the fabric surface.^[17a, 23a, 58] For example, Someya’s group developed the printable and stretchable conductors containing Ag NPs that were in-situ formed by mixing micrometer-sized Ag flakes, fluorine rubbers, and surfactant in the ink (Figure 4i).^[23a] The conductive ink could ensure an initial conductivity of up to 6168 S cm^{-1} and conductivity of 935 S cm^{-1} at 400% strain. Fully printed sensor networks on textile substrates could sense pressure and temperature accurately even when stretched over 250%. Cao et al.^[59] also utilized the CNT ink and screen-printing technology to make electrode patterns on common fabric, which could embrace an electrical conductivity of $200 \text{ } \Omega \text{ sq}^{-1}$, stability under mechanical deformation, and more importantly, the high air permeability (88.2 mm s^{-1}) that was comparable to those of common textiles.

In addition, the laser scribing approach, which is initially used to produce graphene film on polyimide (PI) film, is recently utilized to induce porous graphitized conductive patterns from

textile fabrics.^[60] Tour's group has successfully identified the mechanisms to form laser-induced carbon layers from a variety of carbon resources without severely damaging the mechanical strength of the substrate.^[60a, 60b] Zhang group recently has realized the direct writing of laser-induced graphene with sheet resistance as low as $6 \Omega \text{ sq}^{-1}$ on a Kevlar textile in air and further showed the application of such graphene/Kevlar fabric in wearable Zn-air batteries, ECG electrodes, and NO_2 gas sensors for intelligent protective clothing (Figure 4k-l).^[60d] Further modifying the laser-induced layers on the fabric substrates with organic or inorganic materials by in situ or ex-situ approaches can alter the electronic properties of the conductive patterns, leading to the performance enhancement of such laser-induced compositions for broader electronic applications.^[60c, 60e, 60f]

3.1.3 Nanofiber-mat-based conductors

While fibrous conductors made by the above-mentioned strategies are generally based on fibers with diameters only down to the micrometer range, the recent development of fibers with nanometer-scale dimensions (i.e., nanofibers) has led to the great advancement of new flexible and stretchable conductors.^[61] It is believed that nanofiber mats could have a larger surface-to-volume ratio than the mats made with microfibers. Such high surface area can not only benefit the realization of gas and water permeability but also facilitate the high mass loading of conductive materials, leading to the formation of highly conductive and permeable conductors.^[21c] Electrospinning is one of the most versatile and efficient spinning approaches that can achieve the large-scale production of nanofibers with adjustable diameters ranging from nanometer to micrometer.^[62] Conducting materials can be incorporated into the mats during or after the spinning process to endow the mat with conductivity.^[63] Regarding the applications in flexible and stretchable conductors, electrospun nanofiber mat can be either used as the temporary template for the formation of substrate-free conductive nanostructured networks or served as the flexible/stretchable substrate for permeable conductors.

Nanofiber mat as temporary template

Electrospun nanofiber mats can serve as nanostructured templates for mesh-like metallic flexible/stretchable conductors, in which metallic conductors are firstly introduced onto a soluble nanofiber mat and then the mat will be removed by dissolution. As such, metallic nanostructured mesh networks could be developed for permeable, flexible, and stretchable electronics.^[8a, 64] For example, a transparent metal nanotrough network has been fabricated by depositing a thin layer of metal (e.g., Au, Cu, Ag, Al) on the polyvinyl alcohol (PVA) electrospun nanofiber mat via vacuum deposition. After dissolving the PVA electrospun mat template, the transparent metal nanotrough network can be firmly attached to various substrates including plastic films, paper, and curved glass slides (Figure 5a-c).^[64] The applications of these mesh-like nanostructured metallic conductors in permeable and stretchable on-skin electronics have been recently demonstrated by Someya's group.^[8a] After dissolving the electrospun PVA nanofiber networks, the mesh-like Au conductor could conformably adhere onto the human skin, enabling real-time temperature and pressure sensing as well as the high-precision electromyogram (EMG) recording (Figure 5d-f). Such Au nanomesh could display the maximum tensile strain at 48% and excellent electrical durability: the resistance only increased by 3 times after 10,000 cycles of finger bending (~40% elongation). Notably, the fibrous conductor could present excellent gas and water vapor permeability without blocking sweat evaporation.^[65] Such PVA nanofiber-based temporary templates could also facilitate the bonding of adjacent electrospun mats to form electronic devices with multi-layered configurations (Figure 5g).^[66] Through the dissolution of the PVA nanofibers, the layers could not detach from each other when high pressure of over 100 kPa or repeated rubbing was applied, maintaining its device structure and sensing functionalities for finger pressure monitoring without interference to human sensation (Figure 5h).

Nanofiber mat as flexible/elastic supportive substrates

Elastomeric materials, such as SBS, PU, and PDMS, can be spun into a fiber mat with a porous structure, in which their inherent elastic property can be well retained. As such, the prepared mats can be endowed with air/water permeability, making them suitable for permeable and stretchable electronics. By loading the elastomeric fibers with different types of conductive materials (e.g., metal, carbon-based materials, and conducting polymers) during or after the electrospinning process, permeable and stretchable conductor composites can be obtained, which can be used for epidermal electronics and electronic tattoos (E-tattoo).^[7-8, 20b, 67] For example, metal nanomaterial-based nanofiber mat conductors can be easily achieved by various methods, such as coating, printing, and mixing.^[68] Fan and his colleagues have reported a transparent AgNWs-embedded electrospun polyamine nanofiber mat made by vacuum filtration for epidermal electrodes.^[69] Electrospun nanofiber mat here was employed as the filter and the AgNWs dispersion was vacuum-filtrated onto the mat (Figure 6a). The as-prepared AgNW-embedded nanofiber mat showed a sheet resistance of $8.2 \Omega \text{ sq}^{-1}$ at the optical transparency of 84.9%, and a good air permeability of $6 \text{ cm}^3 \text{ s}^{-1} \text{ cm}^{-2}$. Such electrode mat could conformally bond to various substrates especially the human skin while exhibiting good mechanical durability against 1600 cycles of quick bending (Figure 6b-d). Using biodegradable polymers, such as PVA and poly lactic-co-glycolic acid, as the materials for nanofiber-mat filters, biodegradable and permeable AgNW-embedded nanofiber mats could be obtained (Figure 6e).^[70] They could function as the electrode for the fabrication of TENG-based electronic skins, realizing the real-time and self-powered health and human motion monitoring toward the whole body. Yang and his colleagues reported AgNWs-based breathable electrodes by applying the screen-printing method, in which the AgNWs inks were screen-printed onto the electrospun poly(vinylidene fluoride) nanofiber mats.^[71] The breathable pressure sensor consisting of such screen-printed AgNWs electrode could enable the fast response time ($< 26 \text{ ms}$) to the pressure change, ultralow detection pressure (1.6 Pa), and gas-permeability.

Nanomaterials could also be mixed into the mat during the electrospinning process to allow for a conductive composite nanofiber mat. Fan et al.^[67c] recently reported a hierarchically interactive AgNWs-nanofibers network, which was prepared by simultaneous electrospinning of TPU elastic nanofiber and electrospaying of AgNWs dispersion. This hierarchical structure enabled the composite nanofiber mat to have high conductivity ($4,800 \text{ S cm}^{-1}$), high stretchability (500%), high durability in long-cycle strain deformations (30,000 cycles of 50% strain) and washing test, and more importantly, air permeability of $5.6 \text{ cm}^3 \text{ s}^{-1} \text{ cm}^{-2}$.^[67c] Metallic nanomaterials can be also introduced to electrospun mats by chemical reduction method to form a metallic NPs-based coating. By absorbing the Ag precursor solution into the SBS electrospun nanofiber mat and reducing the absorbed ions with reducing agents, Ag NPs shell could be not only uniformly coating around the fiber surfaces but also inside the fibers of the mat (Figure 6f).^[20b] Due to the conductive percolation networks formed in the nanofiber mat, such AgNPs-coated SBS nanofiber mats presented a high electrical conductivity ($5,400 \text{ S cm}^{-1}$), which could be well maintained during large deformations ($2,200 \text{ S cm}^{-1}$ at 100% strain) (Figure 6g-h).

The methods for incorporating carbon-based materials and conducting polymers with nanofiber mats are similar to those for making metal nanomaterials-based nanofiber-mat conductors.^[67a, 67b, 72] For example, Lu and his colleagues demonstrated an ultrasonication-assisted coating method to achieve the conductive nanofiber composite mats.^[73] Graphene was interspersed and anchored onto the electrospun polyamide 66 nanofibers under the ultrasonic treatment for construct a 3D conductive network in the nanofiber composite mat.^[73b] Such graphene-decorated composite mat could function as the electrodes for ECG, strain, temperature, gas, and moisture measurement. Similarly, Kim's team constructed a skin-adhesive ultrathin E-tattoo via incorporating CNTs onto the ultrathin electrospun silk nanofiber mat. The E-tattoos could be conformably attached to the irregular dermal surface and preserve their functions when mechanical stresses deform the skin, demonstrating their application possibilities for on-skin

diagnostic and therapeutic.^[67d] Jeong et al.^[74] fabricated the breathable, flexible, and biocompatible PEDOT:PSS-based epidermal electrodes for ECG monitoring by spraying the PEDOT:PSS aqueous solution onto the PU electrospun mats (Figure 6g-j). The as-made electrode could exhibit stretchability with a maximum elongation of 30%, high conductivity at 125.4 S m^{-1} , and moisture permeability with a WVTR of about $12 \text{ g m}^{-2} \text{ h}^{-1}$ ($288 \text{ g m}^{-2} \text{ day}^{-1}$) (Figure 6k).

LM could also be utilized to form permeable and stretchable conductors for wearable electronics. Recently, Zheng's group reported the breathable and superelastic LM fibre mats (LMFMs) prepared by electrospinning the elastomeric SBS mats and coating/printing the EGaIn onto the electrospun mats (Figure 7a).^[7] To achieve the permeability of such EGaIn-coated SBS mat, a pre-stretch process was introduced, in which the fiber mat was repeatedly stretched to 1,800% strain for 12 cycles. As such, EGaIn handing among the elastomeric fibers could be self-organized into a laterally mesh-like and vertically buckled structure, simultaneously offering high permeability, stretchability, conductivity, and electrical stability. The air permeability and moisture permeability of the as-developed LMFM were both higher than the commercial nylon cloth and medical patch, which could allow the insensible perspiration of a human body in daily life. Both in vivo animal and on-skin tests showed their breathability and biocompatibility. In addition, the conductivity of such LMFM could reach about $10,000 \text{ S m}^{-1}$ at the released state and its resistance only decreased by 4.1% after stretching to 1,800% strain (Figure 7b). The mat could bear more than 25,000 stretching cycles at 100% strain with a resistance change of less than 30%, which well satisfied the durability requirement for wearable and on-skin electronic applications (Figure 7c-d). Permeable, multifunctional monolithic stretchable electronics have also been demonstrated by using these LMFM as a building block.

3.2 Porous thin-film conductors

Elastomers, such as SBS, PU, and PDMS, are stretchable substrates that have been widely used for soft and wearable electronics.^[2, 4] However, their conventional dense thin-film structure sacrifices their permeability to air/water (WVTR is below $50 \text{ g m}^{-2} \text{ day}^{-1}$), leading to rather poor physiological comfort.^[7] An effective strategy to endow permeability to these thin-film conductors is to engineer their porosity. Through various structure-modified methods, such as kirigami design and templating techniques, pores with controllable sizes ranging from micrometers to millimeters can be created for gas/water penetration, while flexibility/stretchability and conductivity of the conductors can be retained.

3.2.1 Kirigami design

Kirigami, a traditional cutting technique for designing paper-based handiwork, has been employed as a template-free engineering technique to develop stretchable 3D structures for flexible electronics devices.^[19d, 75] Through geometric design and cutting, planar and rigid materials can be directly transformed into 3D out-of-plane deformable forms, which can not only retain the electrical performance but also enhance their conformability toward different shapes.^[76] For example, Chae et al.^[77] demonstrated the breathable and stretchable electrophysiological sensors based on kirigami structures for psychophysiological stress monitoring and human-machine interactions. Au/Ti film was sandwiched by two polyimide films and then was laser-ablated to produce the kirigami spiderweb-like conductive electrode (Figure 8a-b). Owing to the out-of-plane architecture enabled by the kirigami cutting, the type electrodes could exhibit a stretchability of over 95% and a considerable water vapor permeability with WVTR of up to $20 \text{ g m}^{-2} \text{ h}^{-1}$ (Figure 8c-d).

3.2.2 Templating techniques

The fabrication of porous thin-film conductors can also involve templates as porous molds or scaffolds, which can be removed or selectively dissolved to leave the film with mesh/pore structures. For example, Min et al.^[78] reported the highly permeable, stretchable, and adhesive hierarchical mesh-based conductive electrodes by directly pouring the mixture solution of PU and conductive materials (CNT or Ag flakes) onto a PDMS master mold patterned with hexagonal architecture. After solidation, the elastic film patterned with hexagonal mesh structure could be exfoliated from the mold (Figure 8e). Such mesh electrode enabled the water penetration and maintained its electrical conductivity when subjected to 1,000 stretch-release cycles with 100% strain (Figure 8f-g).

In addition, easily dissolved materials, such as salt crystals, sugar cubes, metallic oxide, and ice can be used as sacrificial templates for making porous thin-film conductors.^[79] For example, porous PDMS sponges have been developed by dissolving the cube sugar inside the elastomer matrix.^[80] They can be further endowed with electrical conductivity through PAMD method or vacuum filling of LM.^[80-81] Sun and his colleagues also reported the gas-permeable, multifunctional on-skin bioelectronic sensing system based on the laser-patterned porous graphene as sensing components and the sugar-templated elastomer sponges as stretchable and permeable substrates (Figure 8h-i).^[20a] Such porous materials structure enabled the considerable water vapor permeability ($18 \text{ mg cm}^{-2} \text{ h}^{-1}$), making them preferred for long-term on-skin sensing applications (Figure 8j). The as-developed sensor devices presented the fracture elongation of 330%, which could be further increased to 1,000% by utilizing the kirigami design.

Water droplets could also be utilized as templates to fabricate porous thin-film conductive electrodes. Breath figure is a nature-inspired and self-assembly process, in which water droplets will firstly condensate and then form a water droplet array on a cold surface covered with polymer solution in a highly humid environment. After the evaporation of solvent and water

droplets, a porous film can be attained.^[82] Zhu's group recently demonstrate a gas-permeable, ultrathin, stretchable electrode with porous structure epidermal electronics (Figure 8k-m).^[83] It was prepared by introducing AgNWs into a porous PU film that was made by the breath figure method (Figure 8k). The as-prepared electrode displayed an optical transmittance of 61%, the sheet resistance of $7.3 \Omega \text{ sq}^{-1}$, ultrathin feature with the thickness of only $4.6 \mu\text{m}$, and water vapor permeability with WVTR of $23 \text{ mg cm}^{-2} \text{ h}^{-1}$, which could enable a conformal attachment with the skin to achieve low skin-electrode impedance and high-quality detection of various biopotential signals (Figure 8l-m).

4. Conclusion and Outlook

Permeable conductors are the key building blocks for wearable and on-skin electronics to enable their conformable and comfortable contact with human bodies. In this review, we have discussed three key merits of conductors for wearable and on-skin electronic applications, and have summarized the strategies to develop permeable conductors with flexibility/stretchability both from structural and material viewpoints. To simultaneously render the conductors permeable, conductive, and flexible or stretchable, promising strategies are to construct conducting materials into either fibrous textile formats (i.e, fibers/yarn, fabrics) or elastic films structured engineered with porous architectures. This is because such fibrous and porous configurations can not only ensure sufficient channels for the transmission of gas and liquid within the materials but also provide intrinsic or extrinsic flexibility/stretchability to the as-developed conductors. Recent developed permeable conductors based on these strategies have also been highlighted with the emphasis on their applications of wearable and on-skin electronics. Though many methods have been implemented to enable a large variety of permeable conductors, there remain many challenges that are waiting for further research and development.

One bottleneck is the reliability of the permeable conductors against repeated and large mechanical deformations. It is highly critical for permeable conductors to maintaining stable and reliable conducting performance under different conditions, because various types of mechanical deformations and disruption, including but not limited to bending, folding, stretching, shearing, and abrasion motions, occur frequently and irregularly during the practical wearable and on-skin applications. Other than bending and stretching tests that have been widely implemented for the study of the conductor performance, attention could also be extended to the ability of the permeable conductors to resist friction, shearing, washing, and low/high temperature, which are largely overlooked in the evaluation of conductors. Additional functionalities, such as self-healing, anti-abrasion, waterproof, and thermal stability, thus may be acquired. This will require more understanding of the interplay among materials, structures, and mechanical strains, and the exploitation of new materials and structures with superior mechanical robustness and environmental stability.

Another key development for the future application of on-skin stretchable electronics is the enhancement of the adhesion of conductors to human skins, which can allow for the stable and accurate detection and transmission of body signals. Though recent studies have focused on forming breathable and dry contact between electrodes and human skins via utilizing van der Waals' forces, such type of adhesion mechanism is only effective for extremely thin epidermal electrodes with the thickness below few microns, and a general strategy to build up a strong adhesion between breathable devices and skin that is suitable for a wide range of thickness is still challenging.^[67d, 84] Therefore, further optimization of electrode and device structures is required to balance their adhesion properties and functionalities.^[85] Alternatively, one possible development avenue is the use of hydrogel, which has been attracted great attention as a means of enhancing the adhesion of electrodes due to their biocompatible and viscoelastic features as discussed previously. Via tuning the structures and material compositions, they could be served

as the soft and conformable adhesive layers for flexible and stretchable electronics without affecting their breathability to gas and liquid, preventing damage to human skin and ensuring the steady use of on-skin electronics.

Applications of breathable electronics among long-term healthcare monitoring, human-machine interaction, and energy harvesting have been widely demonstrated based on permeable conductors in research laboratories. However, breathable electronics are still far away from practical applications because of the lack of system integration study and the limitations of scalable fabrication. To date, how to seamlessly integrate different electronic modules, including sensor electrodes, data processing units, and energy harvesting and storage units, into a monolithic patch without affecting the device's functionalities, flexibility/stretchability, and most importantly, permeability is rather challenging. And there are only a few reports on such kinds of highly integrated breathable electronics.^[86] On the other hand, the manufacture of these advanced flexible and stretchable electronics largely involve soft substrate with 1D or 2D architectures, which are not fully compatible with conventional processes for integrated circuit fabrication. In view of these research and development gaps, multidisciplinary studies not only with chemical engineering and mechanical sciences, but also with electronic engineering, system integration, machine learning, and mechanical engineering are highly demanding. With enormous efforts kept investing in materials development, structural designs, fabrication optimization, and system integration, we anticipate that permeable conductors with superior mechanical properties and conductivity could be developed for increasingly practical applications of wearable and on-skin electronic systems.

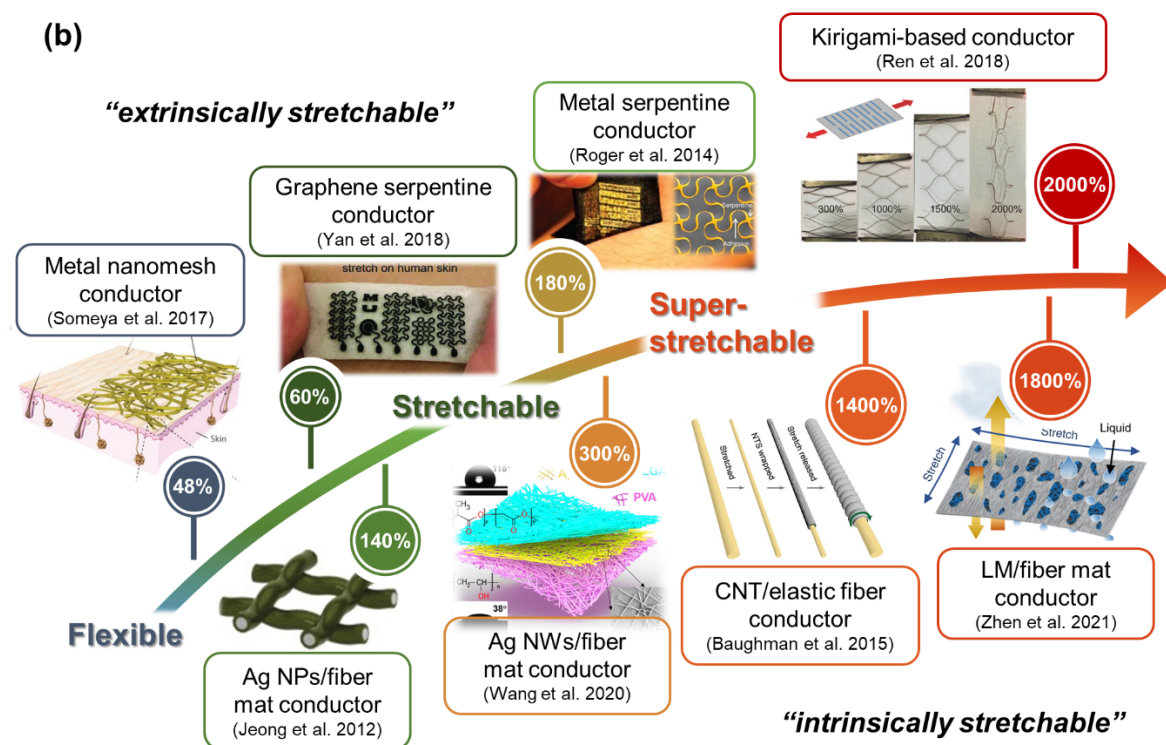
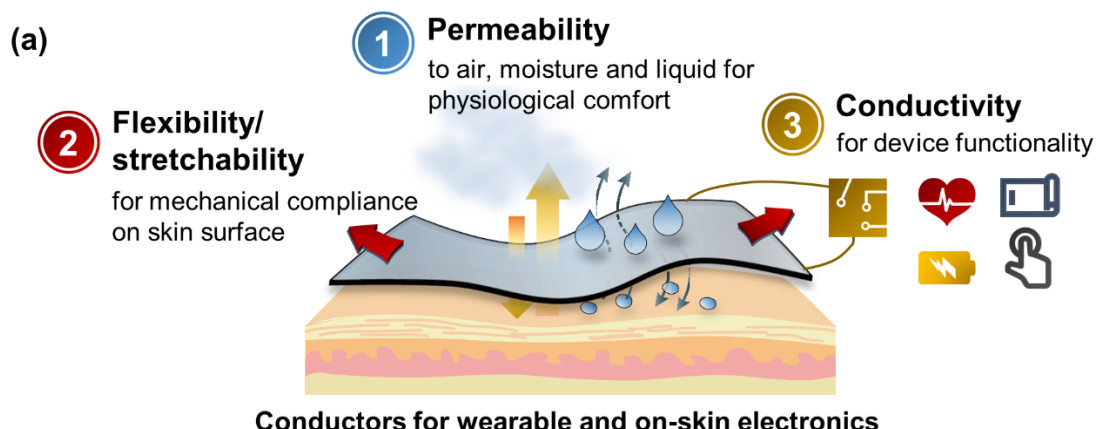


Figure 1. a) Design considerations of conductors for wearable and on-skin electronics: permeability, flexibility/stretchability, and conductivity. b) Development of extrinsically and intrinsically stretchable conductors. Image for “Metal nanomesh conductor”: Reproduced with permission.^[8a] Copyright 2017, Springer Nature. Image for “Graphene serpentine conductor”: Reproduced with permission.^[20a] Copyright 2018, WILEY-VCH. Image for “Metal serpentine conductor”: Reproduced with permission.^[19f] Copyright 2014, Springer Nature. Image for “Kirigami-based conductor”: Reproduced with permission.^[19e] Copyright 2018, WILEY-VCH. Image for “Ag NPs/fiber mat conductor” (Ag NPs: silver nanoparticles) Reproduced with permission.^[20b] Copyright 2012, Springer Nature. Image for “Ag NWs/fiber mat conductor” (Ag NWs: silver nanowires): Reproduced with permission.^[70] Copyright 2020, American

Association for the Advancement of Science. Image for “CNT/elastic fiber conductor”:
Reproduced with permission.^[32f] Copyright 2015, AAAS. Image for “LM/fiber mat conductor”:
Reproduced with permission.^[7] Copyright 2021, Springer Nature.

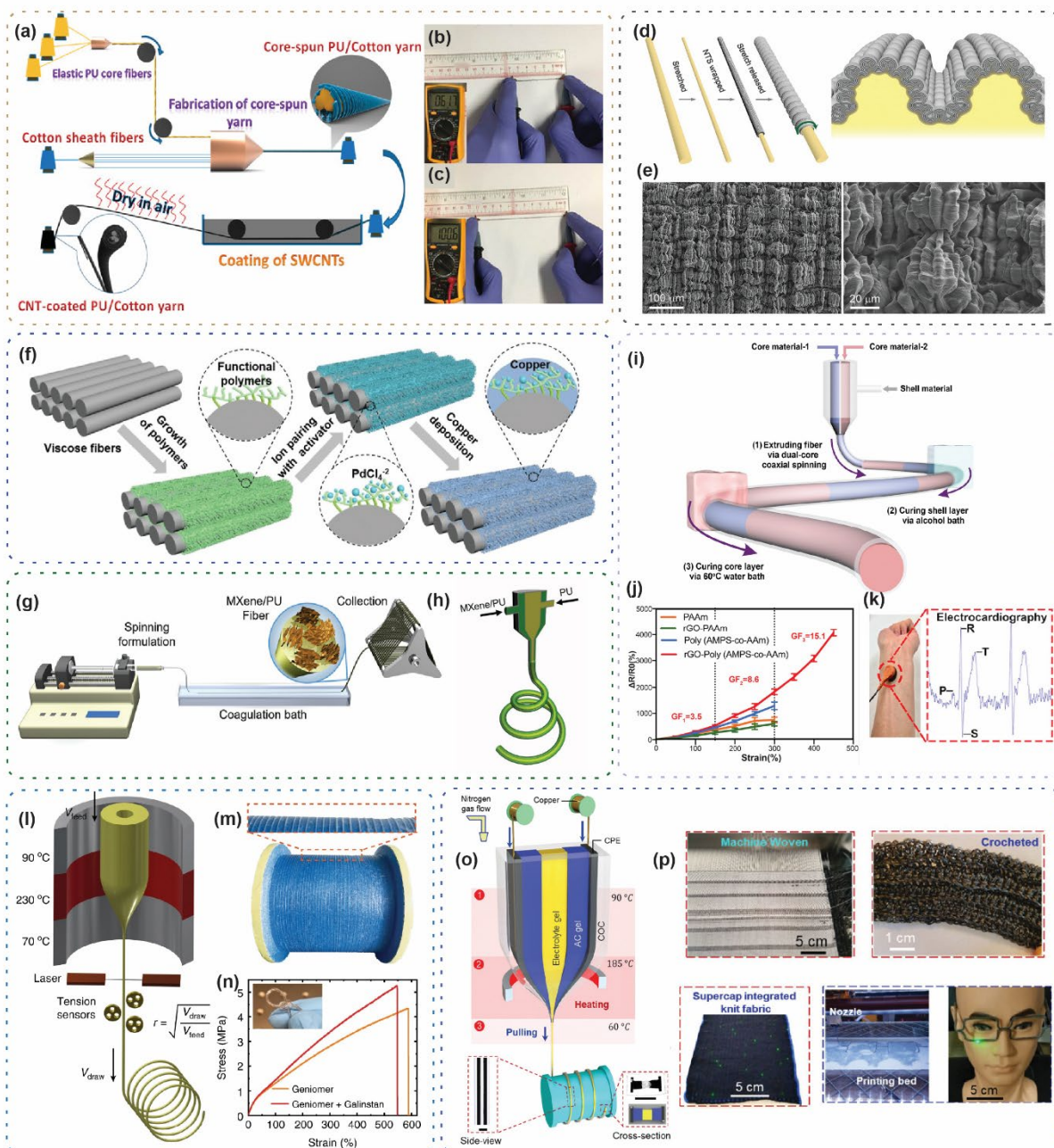


Figure 2. 1D fiber/yarn-shaped conductors achieved by coating or spinning techniques. **a)** Schematic illustration showing the processes for making polyurethane (PU)/Cotton core-spun yarn with carbon nanotube (CNT) coating. **b), c)** Images showing the stretchability of the CNT-coated PU/Cotton yarn and the corresponding electrical resistance change before (b) and after stretching (c). **a-c)** Reproduced with permission.^[32d] Copyright 2016, American Chemical Society. **d)** Left: Fabrication of the CNT-wrapped elastic fibers via “pre-strain” strategy; Right: Illustration showing the two-dimensional hierarchical buckling structure in a longitudinal section of the CNT-wrapped elastic fiber. **e)** Scanning electron microscope (SEM) images showing buckles for CNT-wrapped elastic fiber. **d,e)** Reproduced with permission.^[32f] Copyright 2015, AAAS. **f)** Schematic illustration showing the fabrication of conductive yarn

via polymer-assisted metal deposition approach (PAMD). Reproduced with permission.^[36] Copyright 2021, WILEY-VCH. **g)** Schematic illustration of the spinning process for MXene/PU fiber. **h)** Schematic illustration of the coaxial fiber spinning approach. **g,h)** Reproduced with permission.^[39] Copyright 2020, WILEY-VCH. **i)** Schematic illustration of the spinning process of core-shell segmental fibers. **j)** Resistance changes as a function of the tensile strain of conductive hydrogel fibers. **k)** Application of the conductive hydrogel fiber as electrocardiogram (ECG) electrode. **i-k)** Reproduced with permission.^[45] Copyright 2020, American Chemical Society. **l)** Schematic illustration showing thermal drawing process for the production of long fibers. **m)** Image showing a roll of 40-m stretchable fiber obtained from the drawing process. **n)** Stress-strain curves of fiber without and with an embedded liquid metal electrode. **l-n)** Reproduced with permission.^[47] Copyright 2020, Springer Nature. **o)** Schematic diagram of supercapacitor fiber drawing process. **p)** Demonstration of machine-weaving and 3D printing from thermally drawn supercapacitor fiber. **o,p)** Reproduced with permission.^[49] Copyright 2020, WILEY-VCH.

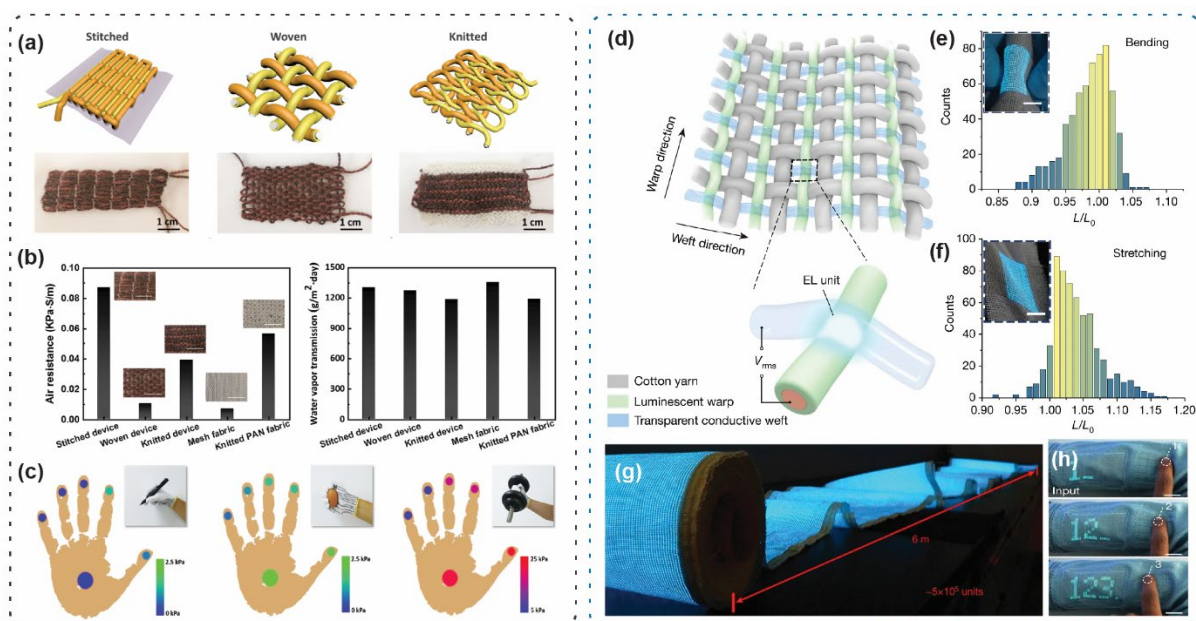


Figure 3. 2D fabric-shaped permeable and flexible/stretchable conductors constructed by weaving approaches. **a)** Schematic illustration (top) and images (bottom) of fabric electrodes constructed by stitching, weaving, and knitting of Cu-PAN (polyacrylonitrile) and parylene-Cu-PAN yarns. **b)** Air resistance (left) and water vapor transmission rate (right) of fabrics with different structures. **c)** Pressure mapping of the pressure sensor made by the stitching of the electrode yarns. **a-c)** Reproduced with permission.^[51] Copyright 2020, Elsevier. **d)** Schematic illustration showing the weave diagram of the display textile. **e), f)** Statistical distribution showing minor variation in luminance for display fabric after 1000 cycles of bending (e) and stretching (f). **g)** Image of 6-m-long display fabrics. **h)** Image of an integrated textile system and its application in human-machine interface. **d-h)** Reproduced with permission.^[3b] Copyright 2021, Springer Nature.

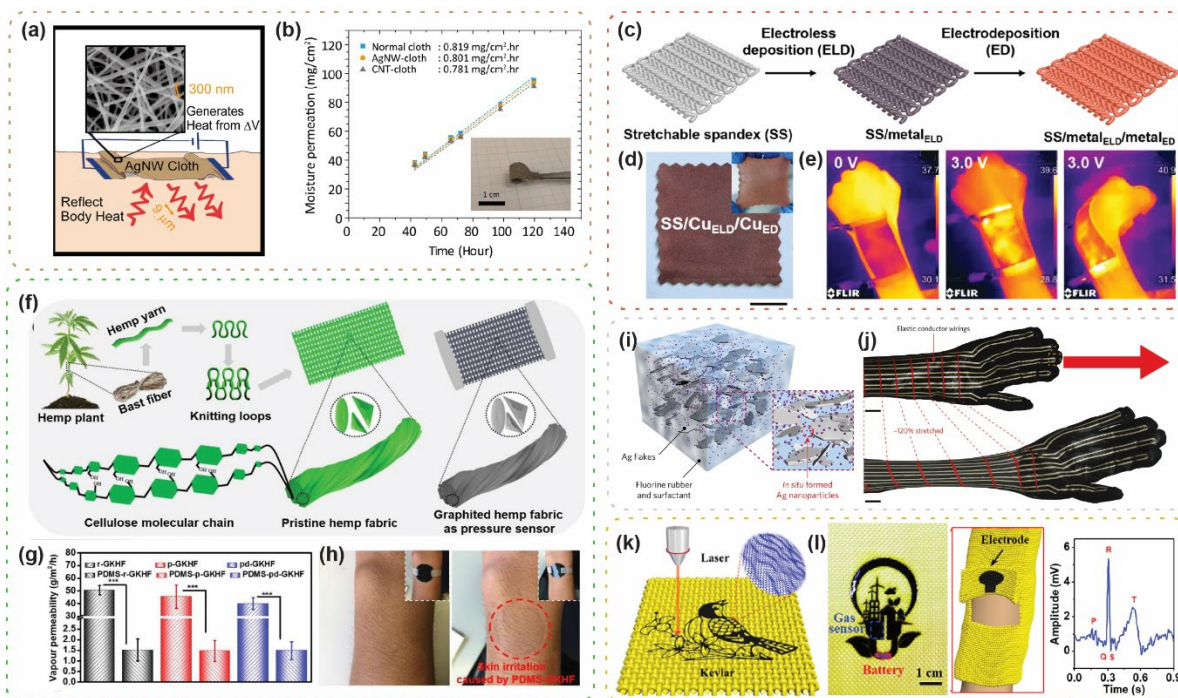


Figure 4. 2D fabric-shaped permeable and flexible/stretchable conductors constructed by coating techniques. **a)** Concept illustration of Ag nanowires (NWs)-coated conductive cloth for thermal radiation insulation and active heating. **b)** Moisture permeation of the cloth samples. Inset is the image showing the flexibility of the AgNW-coated cloth. **a,b)** Reproduced with permission.^[54b] Copyright 2014, American Chemical Society. **c)** Schematic illustration of the fabrication process of metalized stretchable fabric via electroless deposition and electrodeposition. **d)** Image showing the Cu-coated stretchable fabrics. **e)** Application of metalized stretchable fabrics as the wearable heater. **c-e)** Reproduced with permission.^[56a] Copyright 2021, American Chemical Society. **f)** Fabrication of graphite knitted fabrics. **g)** Vapor permeability of the graphite knitted fabrics. **h)** Image before and after attaching breathable graphite knitted fabrics (left) and non-breathable elastic film on the skin. **f-h)** Reproduced with permission.^[57a] Copyright 2021, Elsevier. **i)** Schematic diagram of the structure of printable elastic conductors mixed with Ag nanoparticles (NPs). **j)** Sensor network printed with elastic conductors in the unstretched and 120% stretched conditions. **i,j)** Reproduced with permission.^[23a] Copyright 2017, Springer Nature. **k)** Formation of graphene on Kevlar fabric by laser writing. **l)** Application of laser-scribed conductive fabric electrode in the gas sensor (left) and ECG electrode (right). **k,l)** Reproduced with permission.^[60d] Copyright 2020, American Chemical Society.

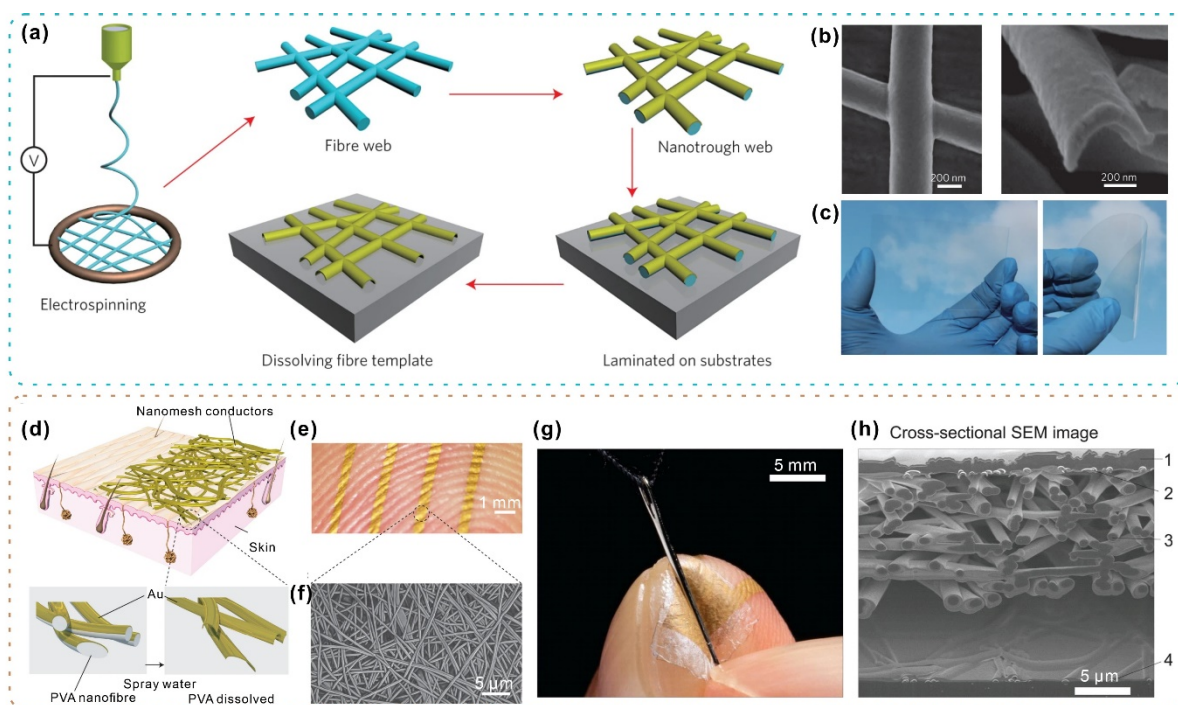


Figure 5. Nanofiber mats as sacrificial templates for constructing permeable and flexible/stretchable conductors. a) Schematic illustration of the fabrication and transfer procedures for metallic nanotrough networks. b) SEM images of the nanotrough network. c) Images showing the nanotrough network transferred onto the glass slide (left) and plastic (right). a-c) Reproduced with permission.^[64] Copyright 2013, Springer Nature. d), e) Schematic illustration (d) and image (e) of the nanomesh attached to the skin made by spraying water on the skin and dissolving the PVA nanofibers. f) SEM image of the nanomesh conductor. d-f) Reproduced with permission.^[8a] Copyright 2017, Springer Nature. g) Image of the nanomesh pressure sensor based on a four-layer structure attached to the skin. h) Cross-sectional SEM image of the nanomesh pressure sensor with the four-layer structure. g,h) Reproduced with permission.^[66] Copyright 2020, AAAS.

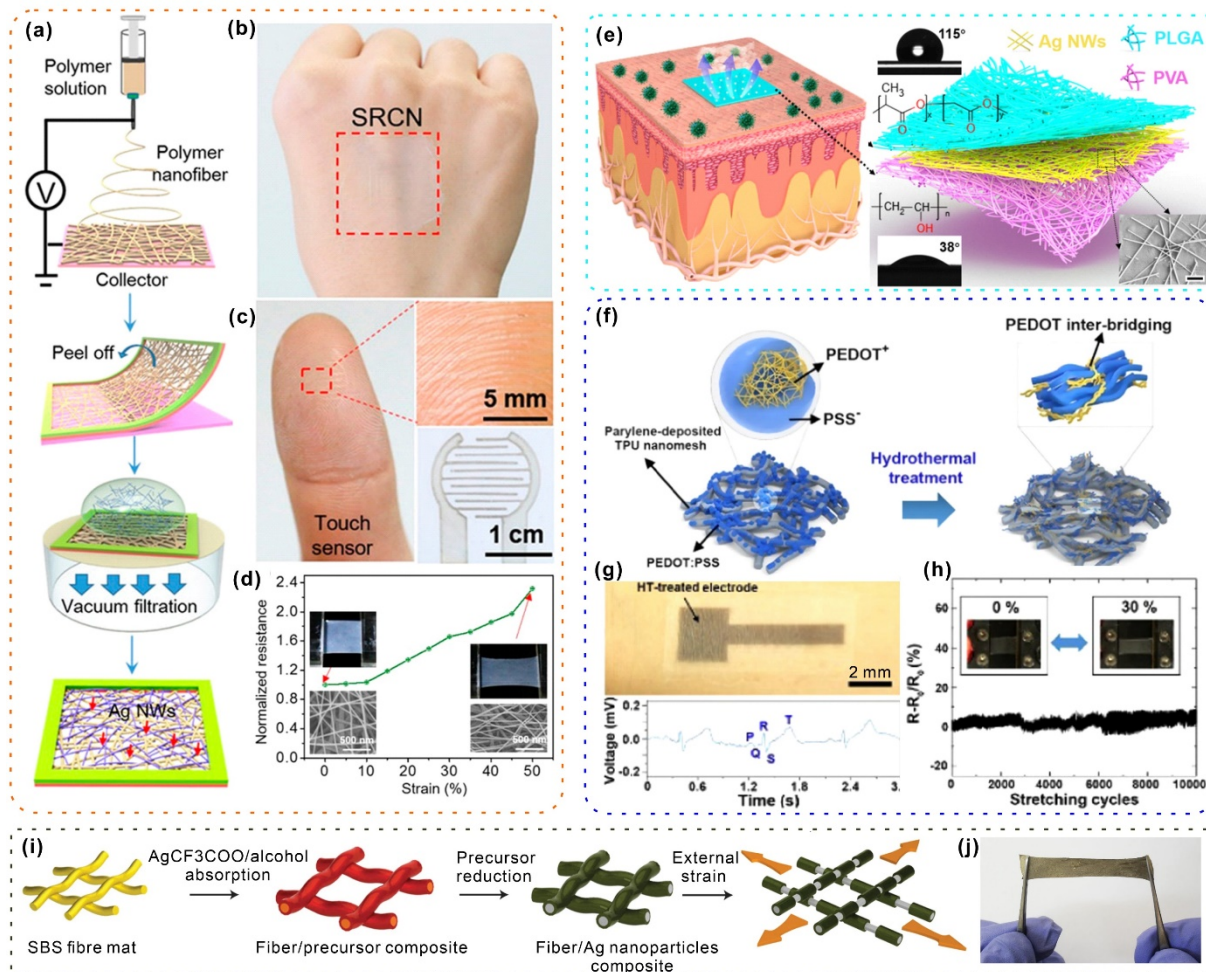


Figure 6. Nanofiber mat-based permeable and flexible/stretchable conductors. **a)** Fabrication process of the AgNWs-based electrospun mat. **b)** Image of the transparent device mounted on the skin. **c)** Image of the touch sensor attached to the fingertip. **d)** Resistance change of the Ag NWs-based electrospun mat as a function of the tensile strain. **a-d)** Reproduced with permission.^[69] Copyright 2018, American Chemical Society. **e)** Schematic illustration of the breathable, degradable, and conductive electronic skin based on a three-layer structure. Reproduced with permission.^[70] Copyright 2020, AAAS. **f)** Schematic illustration of the hydrothermal treatment of the PEDOT:PSS embedded TPU nanomesh. **g)** Image of a hydrothermal-treated electrode mounted on the chest of a person (top) and its use in the real-time monitoring of ECG data (bottom). **h)** Durability of the hydrothermal-treated electrode against loading-unloading cycles at a maximum strain of 30%. **f-h)** Reproduced with permission.^[74] Copyright 2021, American Chemical Society. **i)** Schematic illustration showing the fabrication process of Ag NPs-coated SBS fiber mat through the precursor reduction. **j)** Image of an Ag NPs-coated SBS mat under stretching. **i,j)** Reproduced with permission.^[20b] Copyright 2012, Springer Nature.

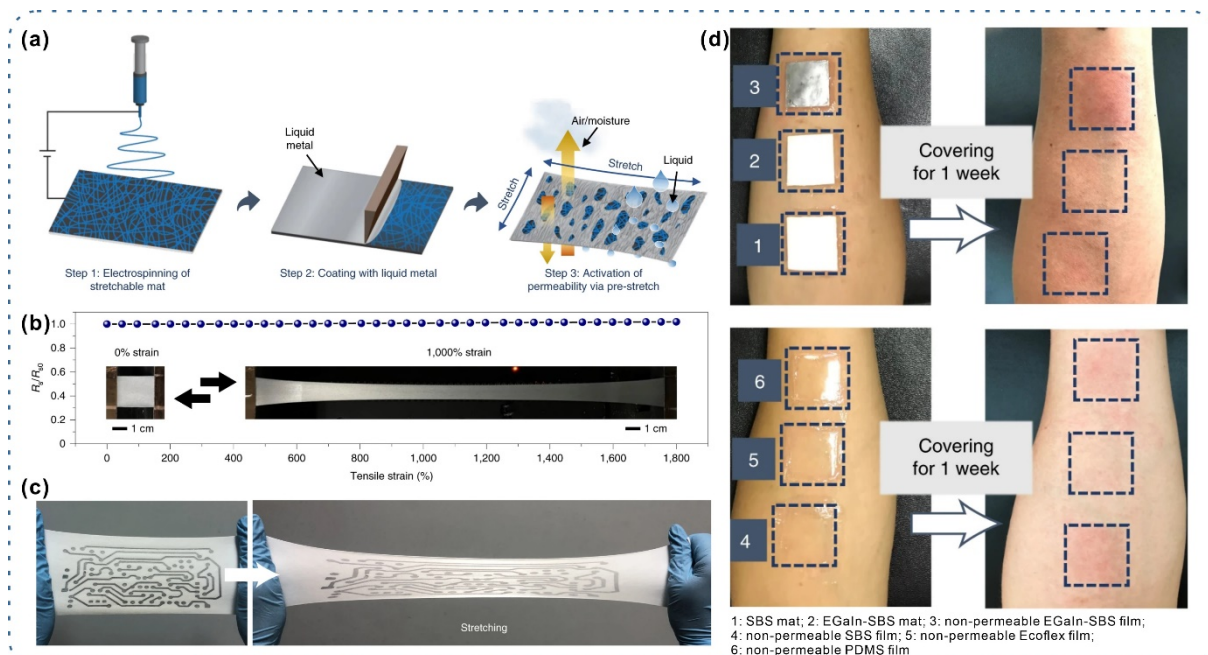


Figure 7. Fabrication of permeable and superelastic fiber mat. **a)** Schematic illustration of the fabrication process of permeable and superelastic liquid-metal fibre mats (LMFMs). **b)** Resistance change of the LMFM as a function of stretching strain. The inset shows the LMFM at a strain of 0% and 1800%. **c)** Images showing the patterned stretchable circuits on the LMFM at the original (left) and the stretching state (right). **d)** Images showing the long-term wearing of LMFM (Sample No. 2). Permeable and superplastic LMFM didn't cause any negative effect on the skin after one week of being attached. Reproduced with permission.^[7] Copyright 2021, Springer Nature.

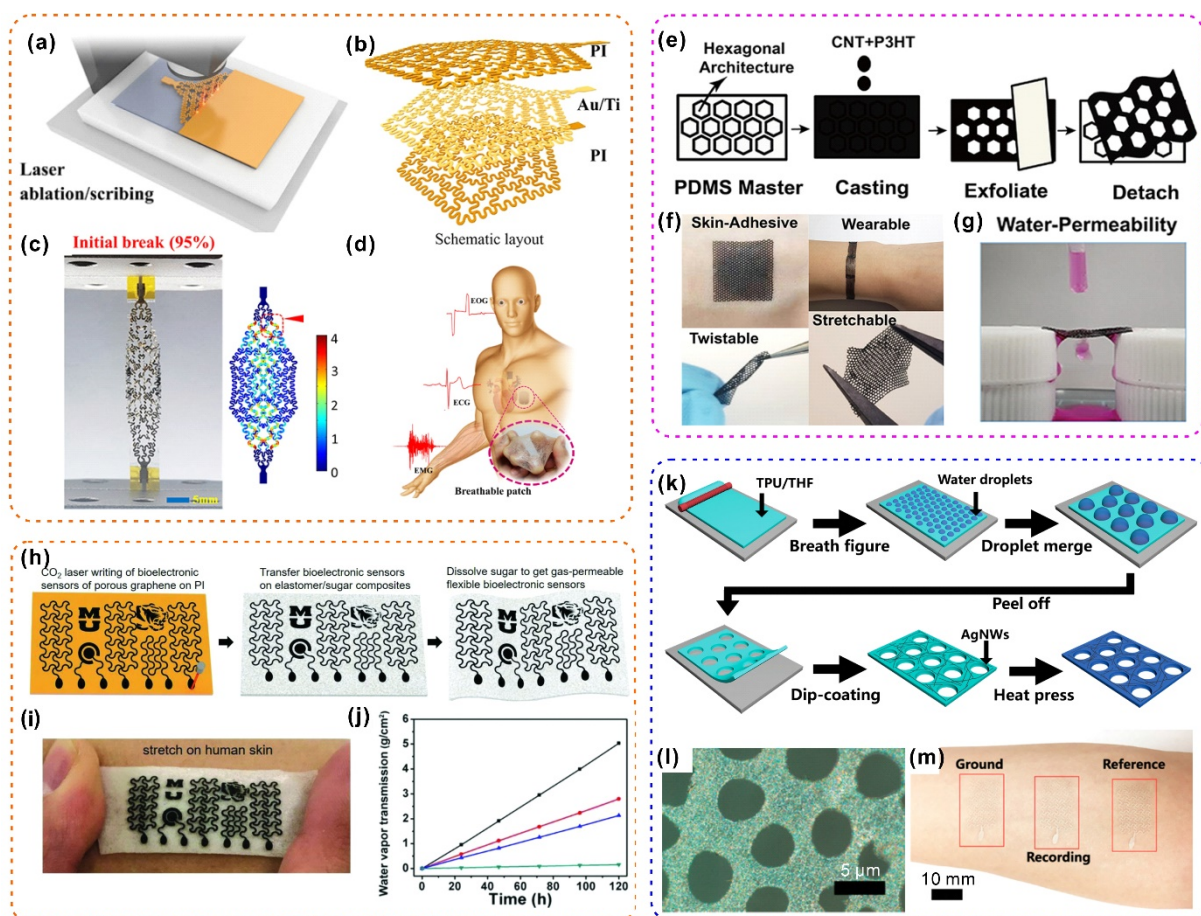


Figure 8. Methods for preparing permeable, stretchable, and conductive porous thin films. **a), b)** Fabrication process (a) and schematic layout (b) of the laser-induced kirigami structures. **c)** Mechanical performance of the kirigami structure at the 95% strain. **d)** Demonstration of the proposed sensors based on the kirigami electrode. **a-d)** Reproduced with permission.^[77] Copyright 2019, American Chemical Society. **e)** Fabrication process for the conductive polymer composite (CPC) film with hexagonal architecture. **f), g)** Demonstration of the skin-adhesive, wearable, twistable, stretchable (f), and water-permeable (g) CPC film. **e-g)** Reproduced with permission.^[78] Copyright 2020, American Chemical Society. **h)** Fabrication process of the PDMS sponges-based biosensors by sugar-templating. **i)** Image of a conductive biosensor stretched on human skin. **j)** Water vapor transmission rate of the biosensors. **h-j)** Reproduced with permission.^[20a] Copyright 2018 WILEY-VCH. **k)** Fabrication process of the porous film based on the breath figure method. **l)** Optical image of the porous film. **m)** Image of the porous film-based electrodes mounted on the forearm for EMG testing. **k-m)** Reproduced with permission.^[83] Copyright 2020, American Chemical Society.

Acknowledgments

Q.H. and F.C. contributed equally to this work. The authors acknowledge the Research Grant Council of Hong Kong (PolyU 153032/18P), Innovation and Technology Fund of Hong Kong (GHP/084/18SZ), and The Hong Kong Polytechnic University Start-up Fund (P0034835) for financial support of this work

Received: ((will be filled in by the editorial staff))

Revised: ((will be filled in by the editorial staff))

Published online: ((will be filled in by the editorial staff))

References

- [1] a) J. A. Rogers; T. Someya; Y. Huang, *Science* **2010**, *327*, 1603; b) Y. Liu; M. Pharr; G. A. Salvatore, *ACS Nano* **2017**, *11*, 9614; c) T. Someya; M. Amagai, *Nat. Biotechnol.* **2019**, *37*, 382; d) J. X. Wang; M. F. Lin; S. Park; P. S. Lee, *Mater. Today* **2018**, *21*, 508.
- [2] N. Matsuhisa; X. Chen; Z. Bao; T. Someya, *Chem. Soc. Rev.* **2019**, *48*, 2946.
- [3] a) D. H. Kim; N. Lu; R. Ma; Y. S. Kim; R. H. Kim; S. Wang; J. Wu; S. M. Won; H. Tao; A. Islam; K. J. Yu; T. I. Kim; R. Chowdhury; M. Ying; L. Xu; M. Li; H. J. Chung; H. Keum; M. McCormick; P. Liu; Y. W. Zhang; F. G. Omenetto; Y. Huang; T. Coleman; J. A. Rogers, *Science* **2011**, *333*, 838; b) X. Shi; Y. Zuo; P. Zhai; J. Shen; Y. Yang; Z. Gao; M. Liao; J. Wu; J. Wang; X. Xu; Q. Tong; B. Zhang; B. Wang; X. Sun; L. Zhang; Q. Pei; D. Jin; P. Chen; H. Peng, *Nature* **2021**, *591*, 240.
- [4] a) C. Wang; C. Wang; Z. Huang; S. Xu, *Adv. Mater.* **2018**, *30*, 1801368; b) D. C. Kim; H. J. Shim; W. Lee; J. H. Koo; D. H. Kim, *Adv. Mater.* **2020**, *32*, 1902743.
- [5] J. Y. Oh; Z. Bao, *Adv. Sci.* **2019**, *6*, 1900186.
- [6] J. Fan, in *Physiological comfort of fabrics and garments*, Vol. (Eds: J. Fan; L. Hunter) Woodhead Publishing, 2009, Ch. 8.
- [7] Z. Ma; Q. Huang; Q. Xu; Q. Zhuang; X. Zhao; Y. Yang; H. Qiu; Z. Yang; C. Wang; Y. Chai; Z. Zheng, *Nat. Mater.* **2021**, *20*, 859.
- [8] a) A. Miyamoto; S. Lee; N. F. Cooray; S. Lee; M. Mori; N. Matsuhisa; H. Jin; L. Yoda; T. Yokota; A. Itoh; M. Sekino; H. Kawasaki; T. Ebihara; M. Amagai; T. Someya, *Nat. Nanotechnol.* **2017**, *12*, 907; b) S. Wei; R. Yin; T. Tang; Y. Wu; Y. Liu; P. Wang; K. Wang; M. Mei; R. Zou; X. Duan, *ACS Nano* **2019**, *13*, 7920.
- [9] R. Matsukawa; A. Miyamoto; T. Yokota; T. Someya, *Adv. Healthc. Mater.* **2020**, *9*, 2001322.
- [10] H.-R. Lim; H. S. Kim; R. Qazi; Y.-T. Kwon; J.-W. Jeong; W.-H. Yeo, *Adv. Mater.* **2020**, *32*, 1901924.
- [11] A. K. Roy Choudhury; P. K. Majumdar; C. Datta, in *Factors affecting comfort: human physiology and the role of clothing*, Vol. (Eds: G. Song) Woodhead Publishing, 2011, Ch. 1.
- [12] S. J. Park; T. Tamura, *Ann. Physiol. Anthropol.* **1992**, *11*, 593.
- [13] Y. Chen; B. Lu; Y. Chen; X. Feng, *Sci. Rep.* **2015**, *5*, 11505.
- [14] a) R. Mishra; J. Militky; M. Venkataraman, in *Nanoporous materials*, Vol. (Eds: R. Mishra; J. Militky) Woodhead Publishing, 2019, Ch. 7; b) L. Hunter; J. Fan, in *Waterproofing and breathability of fabrics and garments*, Vol. (Eds: J. Fan; L.

- Hunter) Woodhead Publishing, 2009, Ch. 11; c) W. Zeng; L. Shu; Q. Li; S. Chen; F. Wang; X. M. Tao, *Adv. Mater.* **2014**, *26*, 5310.
- [15] A. International, in *Standard Test Methods for Water Vapor Transmission of Materials*. ASTM International: West Conshohocken, PA, **2016**; Vol. ASTM E96 / E96M-16.
- [16] A. International, in *Standard Test Method for Air Permeability of Textile Fabrics*. ASTM International: West Conshohocken, PA, **1996**; Vol. ASTM D737-96.
- [17] a) N. Matsuhisa; M. Kaltenbrunner; T. Yokota; H. Jinno; K. Kuribara; T. Sekitani; T. Someya, *Nat. Commun.* **2015**, *6*, 7461; b) Y. Menguc; Y. L. Park; H. Pei; D. Vogt; P. M. Aubin; E. Winchell; L. Fluke; L. Stirling; R. J. Wood; C. J. Walsh, *Int. J. Robot. Res.* **2014**, *33*, 1748.
- [18] a) J. Wang; G. Cai; S. Li; D. Gao; J. Xiong; P. S. Lee, *Adv. Mater.* **2018**, *30*, 1706157; b) Z. F. Liu; S. Fang; F. A. Moura; J. N. Ding; N. Jiang; J. Di; M. Zhang; X. Lepro; D. S. Galvao; C. S. Haines; N. Y. Yuan; S. G. Yin; D. W. Lee; R. Wang; H. Y. Wang; W. Lv; C. Dong; R. C. Zhang; M. J. Chen; Q. Yin; Y. T. Chong; R. Zhang; X. Wang; M. D. Lima; R. Ovalle-Robles; D. Qian; H. Lu; R. H. Baughman, *Science* **2015**, *349*, 400.
- [19] a) D. H. Kim; J. H. Ahn; W. M. Choi; H. S. Kim; T. H. Kim; J. Song; Y. Y. Huang; Z. Liu; C. Lu; J. A. Rogers, *Science* **2008**, *320*, 507; b) S. Xu; Y. Zhang; J. Cho; J. Lee; X. Huang; L. Jia; J. A. Fan; Y. Su; J. Su; H. Zhang; H. Cheng; B. Lu; C. Yu; C. Chuang; T. I. Kim; T. Song; K. Shigeta; S. Kang; C. Dagdeviren; I. Petrov; P. V. Braun; Y. Huang; U. Paik; J. A. Rogers, *Nat. Commun.* **2013**, *4*, 1543; c) T. Someya; Y. Kato; T. Sekitani; S. Iba; Y. Noguchi; Y. Murase; H. Kawaguchi; T. Sakurai, *Proc. Natl. Acad. Sci. U.S.A* **2005**, *102*, 12321; d) L. Xu; T. C. Shyu; N. A. Kotov, *ACS Nano* **2017**, *11*, 7587; e) Y. S. Guan; Z. Zhang; Y. Tang; J. Yin; S. Ren, *Adv. Mater.* **2018**, *30*, 1706390; f) K.-I. Jang; S. Y. Han; S. Xu; K. E. Mathewson; Y. Zhang; J.-W. Jeong; G.-T. Kim; R. C. Webb; J. W. Lee; T. J. Dawidczyk; R. H. Kim; Y. M. Song; W.-H. Yeo; S. Kim; H. Cheng; S. I. Rhee; J. Chung; B. Kim; H. U. Chung; D. Lee; Y. Yang; M. Cho; J. G. Gaspar; R. Carbonari; M. Fabiani; G. Gratton; Y. Huang; J. A. Rogers, *Nat. Commun.* **2014**, *5*, 4779.
- [20] a) B. Sun; R. N. Mccay; S. Goswami; Y. Xu; C. Zhang; Y. Ling; J. Lin; Z. Yan, *Adv. Mater.* **2018**, *30*, 1804327; b) M. Park; J. Im; M. Shin; Y. Min; J. Park; H. Cho; S. Park; M. B. Shim; S. Jeon; D. Y. Chung; J. Bae; J. Park; U. Jeong; K. Kim, *Nat. Nanotechnol.* **2012**, *7*, 803; c) R. Ma; B. Kang; S. Cho; M. Choi; S. Baik, *ACS Nano* **2015**, *9*, 10876.
- [21] a) S. Yao; Y. Zhu, *Adv. Mater.* **2015**, *27*, 1480; b) J. Lee; B. Llerena Zambrano; J. Woo; K. Yoon; T. Lee, *Adv. Mater.* **2020**, *32*, 1902532; c) Y. Wang; T. Yokota; T. Someya, *NPG Asia Mater.* **2021**, *13*, 22.
- [22] Y. Gao; C. Xie; Z. Zheng, *Adv. Energy Mater.* **2021**, *11*, 2002838.
- [23] a) N. Matsuhisa; D. Inoue; P. Zalar; H. Jin; Y. Matsuba; A. Itoh; T. Yokota; D. Hashizume; T. Someya, *Nat. Mater.* **2017**, *16*, 834; b) Y. Wang; C. Zhu; R. Pfattner; H. Yan; L. Jin; S. Chen; F. Molina-Lopez; F. Lissel; J. Liu; N. I. Rabiah; Z. Chen; J. W. Chung; C. Linder; M. F. Toney; B. Murmann; Z. Bao, *Sci. Adv.* **2017**, *3*, 1602076; c) J. Wang; G. Cai; S. Li; D. Gao; J. Xiong; P. S. Lee, *Adv. Mater.* **2018**, *30*, 1706157; d) S. Wang; J. Xu; W. Wang; G. N. Wang; R. Rastak; F. Molina-Lopez; J. W. Chung; S. Niu; V. R. Feig; J. Lopez; T. Lei; S. K. Kwon; Y. Kim; A. M. Foudeh; A. Ehrlich; A. Gasperini; Y. Yun; B. Murmann; J. B. Tok; Z. Bao, *Nature* **2018**, *555*, 83; e) J. Song; S. Chen; L. Sun; Y. Guo; L. Zhang; S. Wang; H. Xuan; Q. Guan; Z. You, *Adv. Mater.* **2020**, *32*, 1906994.
- [24] S. Choi; S. I. Han; D. Kim; T. Hyeon; D. H. Kim, *Chem. Soc. Rev.* **2019**, *48*, 1566.
- [25] J. Le Bideau; L. Viau; A. Vioux, *Chem.Soc.Rev.* **2011**, *40*, 907.

- [26] a) E. Kamio; T. Yasui; Y. Iida; J. P. Gong; H. Matsuyama, *Adv. Mater.* **2017**, *29*, 1704118; b) C. Yang; Z. Suo, *Nat. Rev. Mater.* **2018**, *3*, 125; c) Z. Chen; N. Gao; Y. Chu; Y. He; Y. Wang, *ACS Appl. Mater. Interfaces* **2021**, *13*, 33557.
- [27] a) S. Chen; H.-Z. Wang; R.-Q. Zhao; W. Rao; J. Liu, *Matter* **2020**, *2*, 1446; b) C. Hang; L. Ding; S. Cheng; R. Dong; J. Qi; X. Liu; Q. Liu; Y. Zhang; X. Jiang, *Adv. Mater.* **2021**, *33*, 2101447; c) R. Dong; X. Liu; S. Cheng; L. Tang; M. Chen; L. Zhong; Z. Chen; S. Liu; X. Jiang, *Adv. Healthc. Mater.* **2021**, *10*, 2000641.
- [28] a) M. D. Dickey, *Adv. Mater.* **2017**, *29*, 1606425; b) L. Zhu; B. Wang; S. Handschuh - Wang; X. Zhou, *Small* **2020**, *16*, 1903841.
- [29] a) T. Distler; A. R. Boccaccini, *Acta Biomater.* **2020**, *101*, 1; b) X. Duan; J. Yu; Y. Zhu; Z. Zheng; Q. Liao; Y. Xiao; Y. Li; Z. He; Y. Zhao; H. Wang; L. Qu, *ACS Nano* **2020**, *14*, 14929; c) X. Sun; F. L. Yao; J. J. Li, *J. Mater. Chem. A* **2020**, *8*, 18605; d) Q. Huang; Y. Yang; R. Chen; X. Wang, *EcoMat* **2021**, *3*, e12076.
- [30] a) L. Allison; S. Hoxie; T. L. Andrew, *Chem. Commun.* **2017**, *53*, 7182; b) S. Uzun; S. Seyedin; A. L. Stoltzfus; A. S. Levitt; M. Alhabeib; M. Anayee; C. J. Strobel; J. M. Razal; G. Dion; Y. Gogotsi, *Adv. Funct. Mater.* **2019**, *29*, 1905015.
- [31] a) K. Chatterjee; J. Tabor; T. K. Ghosh, *Fibers* **2019**, *7*, 51; b) J. Lee; H. Kwon; J. Seo; S. Shin; J. H. Koo; C. Pang; S. Son; J. H. Kim; Y. H. Jang; D. E. Kim; T. Lee, *Adv. Mater.* **2015**, *27*, 2433; c) J. Lee; S. Shin; S. Lee; J. Song; S. Kang; H. Han; S. Kim; S. Kim; J. Seo; D. Kim; T. Lee, *ACS Nano* **2018**, *12*, 4259; d) Y. He; Q. Gui; S. Liao; H. Jia; Y. Wang, *Adv. Mater. Technol.* **2016**, *1*.
- [32] a) X. T. Li; H. B. Hu; T. Hua; B. G. Xu; S. X. Jiang, *Nano Res.* **2018**, *11*, 5799; b) Z. Yang; Z. Zhai; Z. Song; Y. Wu; J. Liang; Y. Shan; J. Zheng; H. Liang; H. Jiang, *Adv. Mater.* **2020**, *32*, 1907495; c) J. F. Sun; Y. Huang; C. X. Fu; Z. Y. Wang; Y. Huang; M. S. Zhu; C. Y. Zhi; H. Hu, *Nano Energy* **2016**, *27*, 230; d) Z. Wang; Y. Huang; J. Sun; Y. Huang; H. Hu; R. Jiang; W. Gai; G. Li; C. Zhi, *ACS Appl. Mater. Interfaces* **2016**, *8*, 24837; e) Y. J. Yun; D. Y. Kim; W. G. Hong; D. H. Ha; Y. Jun; H. K. Lee, *RSC Adv.* **2018**, *8*, 7615; f) Z. F. Liu; S. Fang; F. A. Moura; J. N. Ding; N. Jiang; J. Di; M. Zhang; X. Lepró; D. S. Galvão; C. S. Haines; N. Y. Yuan; S. G. Yin; D. W. Lee; R. Wang; H. Y. Wang; W. Lv; C. Dong; R. C. Zhang; M. J. Chen; Q. Yin; Y. T. Chong; R. Zhang; X. Wang; M. D. Lima; R. Ovalle-Robles; D. Qian; H. Lu; R. H. Baughman, *Science* **2015**, *349*, 400; g) Y. He; Q. Gui; S. Liao; H. Jia; Y. Wang, *Adv. Mater. Technol.* **2016**, *1*, 1600170.
- [33] Y. He; Q. Gui; Y. Wang; Z. Wang; S. Liao; Y. Wang, *Small* **2018**, *14*, 1800394.
- [34] a) Y. Yu; C. Yan; Z. Zheng, *Adv. Mater.* **2014**, *26*, 5508; b) P. Li; Y. Zhang; Z. J. Zheng, *Adv. Mater.* **2019**, *31*, 1902987.
- [35] X. Liu; X. Zhou; Y. Li; Z. Zheng, *Chem. Asian J.* **2012**, *7*, 862.
- [36] Z. K. Liu; Y. Zheng; L. Jin; K. L. Chen; H. Zhai; Q. Y. Huang; Z. D. Chen; Y. P. Yi; M. Umar; L. L. Xu; G. Li; Q. W. Song; P. F. Yue; Y. Li; Z. J. Zheng, *Adv. Funct. Mater.* **2021**, *31*, 2007622.
- [37] a) L. Kou; T. Huang; B. Zheng; Y. Han; X. Zhao; K. Gopalsamy; H. Sun; C. Gao, *Nat. Commun.* **2014**, *5*, 3754; b) Q. Q. Zhou; W. L. Teng; Y. H. Jin; L. Sun; P. Hu; H. Y. Li; L. Z. Wang; J. S. Wang, *Electrochim. Acta* **2020**, *334*, 135530.
- [38] a) W. Yan; C. Q. Dong; Y. Z. Xiang; S. Jiang; A. Leber; G. Loke; W. X. Xu; C. Hou; S. F. Zhou; M. Chen; R. Hu; P. P. Shum; L. Wei; X. T. Jia; F. Sorin; X. M. Tao; G. M. Tao, *Mater. Today* **2020**, *35*, 168; b) M. Chen; Z. Wang; K. Li; X. Wang; L. Wei, *Adv. Fiber Mater.* **2021**, *3*, 1.
- [39] S. Seyedin; S. Uzun; A. Levitt; B. Anasori; G. Dion; Y. Gogotsi; J. M. Razal, *Adv. Funct. Mater.* **2020**, *30*, 1910504.
- [40] L. Y. Lan; C. M. Jiang; Y. Yao; J. F. Ping; Y. B. Ying, *Nano Energy* **2021**, *84*, 105954.

- [41] W. Y. Li; Y. F. Zhou; Y. H. Wang; Y. Li; L. Jiang; J. W. Ma; S. J. Chen, *Macromol. Mater. Eng.* **2020**, *305*, 1900736.
- [42] Z. Tang; S. Jia; F. Wang; C. Bian; Y. Chen; Y. Wang; B. Li, *ACS Appl. Mater. Interfaces* **2018**, *10*, 6624.
- [43] J. Zhou; X. Z. Xu; Y. Y. Xin; G. Lubineau, *Adv. Funct. Mater.* **2018**, *28*, 1705591.
- [44] W. Li; Y. Zhou; Y. Wang; L. Jiang; J. Ma; S. Chen; F. L. Zhou, *Adv. Electron. Mater.* **2020**, *7*, 2000865.
- [45] J. Chen; H. Wen; G. Zhang; F. Lei; Q. Feng; Y. Liu; X. Cao; H. Dong, *ACS Appl. Mater. Interfaces* **2020**, *12*, 7565.
- [46] a) A. Leber; C. Q. Dong; R. Chandran; T. Das Gupta; N. Bartolomei; F. Sorin, *Nat. Electron.* **2020**, *3*, 316; b) Y. Qu; T. Nguyen-Dang; A. G. Page; W. Yan; T. Das Gupta; G. M. Rotaru; R. M. Rossi; V. D. Favrod; N. Bartolomei; F. Sorin, *Adv. Mater.* **2018**, *30*, 1707251; c) M. Bayindir; F. Sorin; A. F. Abouraddy; J. Viens; S. D. Hart; J. D. Joannopoulos; Y. Fink, *Nature* **2004**, *431*, 826.
- [47] C. Dong; A. Leber; T. Das Gupta; R. Chandran; M. Volpi; Y. Qu; T. Nguyen-Dang; N. Bartolomei; W. Yan; F. Sorin, *Nat. Commun.* **2020**, *11*, 3537.
- [48] a) T. Khudiyev; C. Hou; A. M. Stolyarov; Y. Fink, *Adv. Mater.* **2017**, *29*, 1605868; b) A. F. Abouraddy; M. Bayindir; G. Benoit; S. D. Hart; K. Kuriki; N. Orf; O. Shapira; F. Sorin; B. Temelkuran; Y. Fink, *Nat. Mater.* **2007**, *6*, 336.
- [49] T. Khudiyev; J. T. Lee; J. R. Cox; E. Argentieri; G. Loke; R. Yuan; G. H. Noel; R. Tataru; Y. Yu; F. Logan; J. Joannopoulos; Y. Shao-Horn; Y. Fink, *Adv. Mater.* **2020**, *32*, 2004971.
- [50] a) J. Shi; S. Liu; L. Zhang; B. Yang; L. Shu; Y. Yang; M. Ren; Y. Wang; J. Chen; W. Chen; Y. Chai; X. Tao, *Adv. Mater.* **2020**, *32*, 1901958; b) C. J. Li; R. Cao; X. L. Zhang, *Appl. Sci.* **2018**, *8*, 2485; c) X. Y. Guan; B. G. Xu; M. J. Wu; T. T. Jing; Y. J. Yang; Y. Y. Gao, *Nano Energy* **2021**, *80*, 105549.
- [51] Z. Z. Zhao; Q. Y. Huang; C. Yan; Y. D. Liu; X. W. Zeng; X. D. Wei; Y. F. Hu; Z. J. Zheng, *Nano Energy* **2020**, *70*, 104528.
- [52] a) M. S. Sadi; J. J. Pan; A. C. Xu; D. S. Cheng; G. M. Cai; X. Wang, *Cellulose* **2019**, *26*, 7569; b) M. Pasta; F. La Mantia; L. B. Hu; H. D. Deshazer; Y. Cui, *Nano Res.* **2010**, *3*, 452; c) L. Hu; M. Pasta; F. L. Mantia; L. Cui; S. Jeong; H. D. Deshazer; J. W. Choi; S. M. Han; Y. Cui, *Nano Lett.* **2010**, *10*, 708.
- [53] a) N. Karim; S. Afroj; S. Tan; P. He; A. Fernando; C. Carr; K. S. Novoselov, *ACS Nano* **2017**, *11*, 12266; b) G. M. Cai; Z. L. Xu; M. Y. Yang; B. Tang; X. G. Wang, *Appl. Surf. Sci.* **2017**, *393*, 441; c) L. V. Thekkekara; M. Gu, *Sci. Rep.* **2019**, *9*, 11822.
- [54] a) M. Sala De Medeiros; D. Chanci; C. Moreno; D. Goswami; R. V. Martinez, *Adv. Funct. Mater.* **2019**, *29*, 1904350; b) P. C. Hsu; X. Liu; C. Liu; X. Xie; H. R. Lee; A. J. Welch; T. Zhao; Y. Cui, *Nano Lett.* **2015**, *15*, 365.
- [55] J. Xu; D. X. Wang; Y. Yuan; W. Wei; S. J. Gu; R. N. Liu; X. J. Wang; L. Liu; W. L. Xu, *Cellulose* **2015**, *22*, 1355.
- [56] a) X. Lu; W. H. Shang; G. K. Chen; H. F. Wang; P. Tan; X. B. Deng; H. F. Song; Z. Y. Xu; J. Q. Huang; X. C. Zhou, *ACS Appl. Electron. Mater.* **2021**, *3*, 1477; b) X. Lin; M. M. Wu; L. Zhang; D. R. Wang, *ACS Appl. Electron. Mater.* **2019**, *1*, 397; c) S. Yang; S. Liu; X. J. Ding; B. Zhu; J. D. Shi; B. Yang; S. R. Liu; W. Chen; X. M. Tao, *Compos. Sci. Technol.* **2021**, *207*, 108729.
- [57] a) Z. K. Liu; K. L. Chen; A. Fernando; Y. Gao; G. Li; L. Jin; H. Zhai; Y. P. Q. Yi; L. L. Xu; Y. Zheng; H. X. Li; Y. Y. Fan; Y. Li; Z. J. Zheng, *Chem. Eng. J.* **2021**, *403*, 126191; b) C. Wang; X. Li; E. Gao; M. Jian; K. Xia; Q. Wang; Z. Xu; T. Ren; Y. Zhang, *Adv. Mater.* **2016**, *28*, 6640; c) W. He; C. Wang; H. Wang; M. Jian; W. Lu; X. Liang; X. Zhang; F. Yang; Y. Zhang, *Sci. Adv.* **2019**, *5*, eaax0649; d) S. Y. You; Y. H.

- Park; C. R. Park, *Carbon* **2000**, *38*, 1453; e) L. Bao; X. Li, *Adv. Mater.* **2012**, *24*, 3246.
- [58] a) K. Jost; D. Stenger; C. R. Perez; J. K. McDonough; K. Lian; Y. Gogotsi; G. Dion, *Energy Environ. Sci.* **2013**, *6*, 2698; b) Y. Chen; Z. Deng; R. Ouyang; R. Zheng; Z. Jiang; H. Bai; H. Xue, *Nano Energy* **2021**, *84*, 105866; c) I. Kim; H. Shahariar; W. F. Ingram; Y. Zhou; J. S. Jur, *Adv. Funct. Mater.* **2019**, *29*, 1807573.
- [59] R. Cao; X. Pu; X. Du; W. Yang; J. Wang; H. Guo; S. Zhao; Z. Yuan; C. Zhang; C. Li; Z. L. Wang, *ACS Nano* **2018**, *12*, 5190.
- [60] a) J. Lin; Z. Peng; Y. Liu; F. Ruiz-Zepeda; R. Ye; E. L. Samuel; M. J. Yacaman; B. I. Yakobson; J. M. Tour, *Nat. Commun.* **2014**, *5*, 5714; b) Y. Chyan; R. Ye; Y. Li; S. P. Singh; C. J. Armusch; J. M. Tour, *ACS Nano* **2018**, *12*, 2176; c) Y. Miao; L. J. Wan; X. F. Ling; B. Chen; L. K. Pan; Y. Gao, *ACS Appl. Electron. Mater.* **2020**, *2*, 855; d) H. Wang; H. Wang; Y. Wang; X. Su; C. Wang; M. Zhang; M. Jian; K. Xia; X. Liang; H. Lu; S. Li; Y. Zhang, *ACS Nano* **2020**, *14*, 3219; e) W. Liu; Y. H. Huang; Y. D. Peng; M. Walczak; D. Wang; Q. Chen; Z. Liu; L. Li, *ACS Appl. Nano Mater.* **2020**, *3*, 283; f) R. Ye; D. K. James; J. M. Tour, *Adv. Mater.* **2019**, *31*, 1803621.
- [61] Q. Y. Huang; D. R. Wang; Z. J. Zheng, *Adv. Energy Mater.* **2016**, *6*, 1600783.
- [62] a) A. Greiner; J. H. Wendorff, *Angew. Chem. Int. Ed.* **2007**, *46*, 5670; b) J. Xue; J. Xie; W. Liu; Y. Xia, *Acc. Chem. Res.* **2017**, *50*, 1976.
- [63] J. Xue; T. Wu; Y. Dai; Y. Xia, *Chem. Rev.* **2019**, *119*, 5298.
- [64] H. Wu; D. Kong; Z. Ruan; P. C. Hsu; S. Wang; Z. Yu; T. J. Carney; L. Hu; S. Fan; Y. Cui, *Nat. Nanotechnol.* **2013**, *8*, 421.
- [65] Y. Wang; S. Lee; T. Yokota; H. Wang; Z. Jiang; J. Wang; M. Koizumi; T. Someya, *Sci. Adv.* **2020**, *6*, eabb7043.
- [66] S. Lee; S. Franklin; F. A. Hassani; T. Yokota; M. O. G. Nayeem; Y. Wang; R. Leib; G. Cheng; D. W. Franklin; T. Someya, *Science* **2020**, *370*, 966.
- [67] a) Q. Pan; N. Tong; N. He; Y. Liu; E. Shim; B. Pourdeyhimi; W. Gao, *ACS Appl. Mater. Interfaces* **2018**, *10*, 7927; b) L. Lan; J. Xiong; D. Gao; Y. Li; J. Chen; J. Lv; J. Ping; Y. Ying; P. S. Lee, *ACS Nano* **2021**, *15*, 5307; c) Y. J. Fan; P. T. Yu; F. Liang; X. Li; H. Y. Li; L. Liu; J. W. Cao; X. J. Zhao; Z. L. Wang; G. Zhu, *Nanoscale* **2020**, *12*, 16053; d) N. Gogurla; Y. Kim; S. Cho; J. Kim; S. Kim, *Adv. Mater.* **2021**, *33*, 2008308.
- [68] T. Sanniccolo; M. Lagrange; A. Cabos; C. Celle; J.-P. Simonato; D. Bellet, *Small* **2016**, *12*, 6052.
- [69] Y. J. Fan; X. Li; S. Y. Kuang; L. Zhang; Y. H. Chen; L. Liu; K. Zhang; S. W. Ma; F. Liang; T. Wu; Z. L. Wang; G. Zhu, *ACS Nano* **2018**, *12*, 9326.
- [70] X. Peng; K. Dong; C. Ye; Y. Jiang; S. Zhai; R. Cheng; D. Liu; X. Gao; J. Wang; Z. L. Wang, *Sci. Adv.* **2020**, *6*, eaba9624.
- [71] W. Yang; N. W. Li; S. Y. Zhao; Z. Q. Yuan; J. N. Wang; X. Y. Du; B. Wang; R. Cao; X. Y. Li; W. H. Xu; Z. L. Wang; C. J. Li, *Adv. Mater. Technol.* **2018**, *3*, 1700241.
- [72] a) K. M. Shi; B. Sun; X. Y. Huang; P. K. Jiang, *Nano Energy* **2018**, *52*, 153; b) K. Saetia; J. M. Schnorr; M. M. Mannarino; S. Y. Kim; G. C. Rutledge; T. M. Swager; P. T. Hammond, *Adv. Funct. Mater.* **2014**, *24*, 492; c) O. Y. Kweon; S. J. Lee; J. H. Oh, *NPG Asia Mater.* **2018**, *10*, 540.
- [73] a) L. J. Lu; B. Yang; J. Q. Liu, *Chem. Eng. J.* **2020**, *400*, 125928; b) L. Lu; C. Jiang; G. Hu; J. Liu; B. Yang, *Adv. Mater.* **2021**, *33*, 2100218.
- [74] W. Jeong; Y. Park; G. Gwon; J. Song; S. Yoo; J. Bae; Y. H. Ko; J. H. Choi; S. Lee, *ACS Appl. Mater. Interfaces* **2021**, *13*, 5660.
- [75] Z. Wang; X. Li; Z. Yang; H. Guo; Y. J. Tan; G. J. Susanto; W. Cheng; W. Yang; B. C. K. Tee, *EcoMat* **2021**, *3*, e12073.

- [76] a) M. K. Bles; A. W. Barnard; P. A. Rose; S. P. Roberts; K. L. McGill; P. Y. Huang; A. R. Ruyack; J. W. Kevek; B. Kobrin; D. A. Muller; P. L. Mceuen, *Nature* **2015**, 524, 204; b) R. Ma; C. Wu; Z. L. Wang; V. V. Tsukruk, *ACS Nano* **2018**, 12, 9714; c) B. M. Li; I. Kim; Y. Zhou; A. C. Mills; T. J. Flewellin; J. S. Jur, *Adv. Mater. Technol.* **2019**, 4, 1900511; d) R. Zhao; S. Lin; H. Yuk; X. Zhao, *Soft Matter* **2018**, 14, 2515.
- [77] H. Chae; H. J. Kwon; Y. K. Kim; Y. Won; D. Kim; H. J. Park; S. Kim; S. Gandla, *ACS Appl. Mater. Interfaces* **2019**, 11, 28387.
- [78] H. Min; S. Jang; D. W. Kim; J. Kim; S. Baik; S. Chun; C. Pang, *ACS Appl. Mater. Interfaces* **2020**, 12, 14425.
- [79] D. Zhu; S. Handschuh-Wang; X. Zhou, *J. Mater. Chem. A* **2017**, 5, 16467.
- [80] S. Q. Liang; Y. Y. Li; Y. Z. Chen; J. B. Yang; T. P. Zhu; D. Y. Zhu; C. X. He; Y. Z. Liu; S. Handschuh-Wang; X. C. Zhou, *J. Mater. Chem. C* **2017**, 5, 1586.
- [81] S. Liang; Y. Li; J. Yang; J. Zhang; C. He; Y. Liu; X. Zhou, *Adv. Mater. Technol.* **2016**, 1, 1600117.
- [82] a) A. Zhang; H. Bai; L. Li, *Chem. Rev.* **2015**, 115, 9801; b) X. Zhang; B. Wang; L. Huang; W. Huang; Z. Wang; W. Zhu; Y. Chen; Y. Mao; A. Facchetti; T. J. Marks, *Sci. Adv.* **2020**, 6, eaaz1042.
- [83] W. Zhou; S. Yao; H. Wang; Q. Du; Y. Ma; Y. Zhu, *ACS Nano* **2020**, 14, 5798.
- [84] a) J. Deng; H. Yuk; J. Wu; C. E. Varela; X. Chen; E. T. Roche; C. F. Guo; X. Zhao, *Nat. Mater.* **2021**, 20, 229; b) D.-H. Kim; J. Viventi; J. J. Amsden; J. Xiao; L. Vigeland; Y.-S. Kim; J. A. Blanco; B. Panilaitis; E. S. Frechette; D. Contreras; D. L. Kaplan; F. G. Omenetto; Y. Huang; K.-C. Hwang; M. R. Zakin; B. Litt; J. A. Rogers, *Nat. Mater.* **2010**, 9, 511; c) Y. Wang; Y. Qiu; S. K. Ameri; H. Jang; Z. Dai; Y. Huang; N. Lu, *npj Flex. Electron.* **2018**, 2, 6; d) S. Kabiri Ameri; R. Ho; H. Jang; L. Tao; Y. Wang; L. Wang; D. M. Schnyer; D. Akinwande; N. Lu, *ACS Nano* **2017**, 11, 7634.
- [85] X. Liu; L. Shi; X. Wan; B. Dai; M. Yang; Z. Gu; X. Shi; L. Jiang; S. Wang, *Adv. Mater.* **2021**, 33, 2007301.
- [86] a) H. Zhang; R. He; H. Liu; Y. Niu; Z. Li; F. Han; J. Li; X. Zhang; F. Xu, *Sens. Actuator A Phys.* **2021**, 322, 112611; b) Y.-T. Kwon; J. J. Norton; A. Cutrone; H.-R. Lim; S. Kwon; J. J. Choi; H. S. Kim; Y. C. Jang; J. R. Wolpaw; W.-H. Yeo, *Biosens. Bioelectron.* **2020**, 165, 112404.

Author Photograph



Fan Chen is a Ph.D. candidate under the supervision of Prof. Zijian Zheng in the Institute of Textiles and Clothing at The Hong Kong Polytechnic University. He received his B.Eng. (2017) in chemical engineering and technology from Hunan University of Science and Technology and M.Sc. (2020) in chemical engineering from Shenzhen University in China. His research interests include polymer, soft and wearable electronics, and human-electronics interfaces.



Qiyao Huang is currently Research Assistant Professor at the Hong Kong Polytechnic University. She received her B.A. in Fashion and Textiles (2014) and Ph.D. (2019) in Textile Technology from The Hong Kong Polytechnic University. After a postdoctoral stay in Prof. Zijian Zheng's group, she joined the Institute of Textiles and Clothing at The Hong Kong Polytechnic University as a Research Assistant Professor in 2020. Her research interests include conductive textiles, flexible and stretchable electrodes and devices for electrochemical energy storage and sensing applications.



Zijian Zheng is a full professor at the Institute of Textiles and Clothing at The Hong Kong Polytechnic University. He received his B.Eng. degree (2003) in chemical engineering at Tsinghua University, Ph.D. degree (2007) in chemistry and nanoscience at the University of Cambridge, and postdoctoral training at Northwestern University between 2008 and 2009. His research interests include surface and polymer science, nanofabrication, flexible and wearable materials and devices, and energy. He is elected as Founding Member of The Young Academy of Sciences of Hong Kong.

In this review article, key design considerations for developing conductors for wearable and on-skin electronics are discussed. The state-of-the-art strategies to simultaneously enable the conductors conductive, flexible or stretchable, and permeable to air, moisture, and liquid are summarised. Challenges and prospects of permeable electronics are also discussed in this review.

Fan Chen[#], Qiyao Huang^{#*}, and Zijian Zheng^{*}

Permeable conductors for wearable and on-skin electronics

